April 2015

Quantifying Ski Edge Curvature

John Joseph Foody
Worcester Polytechnic Institute

Patrick John Wall
Worcester Polytechnic Institute

Richard Reeves Malcolm
Worcester Polytechnic Institute

Samuel Scott Hastings
Worcester Polytechnic Institute

Tina Marissa Dutra
Worcester Polytechnic Institute

Project Number: ME-CAB-1503

Quantifying Ski Edge Curvature

A Major Qualifying Project Report
Submitted to the Faculty
of the
WORCESTER POLYTECHNIC INSTITUTE
in partial fulfillment of the requirements for the
Degree of Bachelor of Science
in Mechanical Engineering
by

Tina M. Dutra
John J. Foody
Samuel S. Hastings
Richard R. Malcolm
Patrick J. Wall

Date: 30 April 2015

Approved:

_____

Prof. Christopher A. Brown, Major Advisor

Abstract

Using axiomatic design, this group designed a device to measure the sharpness of ski edges. Because no quantifiable methods currently exist, we conducted our own research to define the relationship between an edge's curvature and its performance. We defined performance as an edge's ability to hold against a material under simultaneous normal and tangential loads. Using profiles extracted from a 3D topographic measurement, the curvatures of our steel edge samples were calculated as a function of scale and position using Heron's method. In our analysis we discovered the optimal range of scales to observe ski edge curvatures and used our results to design a portable device for skiers to check their edge quality. The device's final design utilized an optical method to measure an edge by extracting the curvature from the distortion of a projected line.

Table of Contents

Table of Figures

Acknowledgements:

We would like to thank the following people for their contributions to our project:

Professor Christopher A. Brown

Professor Cosme Furlong-Vazquez

Morteza Khakeghi Meybodi

Matthew A. Gleason

Tomasz Bartkowiak

WPI Surface Metrology Laboratory Staff

1. Introduction

Ski racing is an intense sport that requires sharp focus and reliable equipment that enables a racer to turn quickly and accurately. To ski the fastest route down a course, a racer must take the tightest turns possible around course markers. Having properly tuned edges enhances the skier's ability to carve a path and reduce the amount of speed lost in each turn. Ski tuning is an essential part of skiing, yet little quantifiable information is known about ski edges. Professional tuners rely heavily on their personal experience and knowledge of snow conditions to decide how to correctly tune a ski for its desired usage.

1.1. Objective

The objective of this Major Qualifying Project (MQP) is to design a portable device to quantify the sharpness of a ski edge by measuring it's curvature at incremental points down the length of the ski.

1.2. Rationale

According to SnowSports Industries America, there are an estimated 16,343,000 alpine skiers and snowboarders in the United States (*2015 SIA Snow Sports Fact Sheet*, 2015). Avid tuners and ski racers in this demographic could integrate this device into their daily tuning routine as a quality check to optimize ski edge sharpness for projected snow conditions. For retail shops and ski and snowboard manufacturers, this device could be used as a quality check to insure that skis are being sharpened to satisfactory. This device could also help mitigate risk of injury by allowing the user to identify when their skis need to be sharpened.

1.3. State of the Art

Currently, the most widely used technique to test ski edge sharpness is the fingernail test. In this quick test, one lightly runs his or her fingernail across the ski edge perpendicular to the running length of the ski. The idea is a sharp ski will remove some of the tester's nail in the form of shavings. If the edge does not remove any fingernail material, then the edge is dull and needs sharpening (Bruton et al., 2013).

Recently, the company Ski Visions developed the Tuning Stick to test the sharpness of ski edges. The Tuning Stick is a hard plastic rod used similarly to the fingernail test. The makers claim that it is more reliable because it is more repeatable. To test the sharpness of a ski edge with the Tuning Stick, the user must hold the tuning stick at a 45 degree angle to the edge and use a moderate amount of pressure to push the plastic stick across the ski edge. Based on the shavings produced, the vibrations of the stick, and the sound the stick produces, the tuner can make a more educated assessment of ski edge sharpness. A sharp and polished ski will produce smooth and consistent shavings, while a sharp ski with a burred edge will vibrate and make a squealing sound (Sewell, 2014).

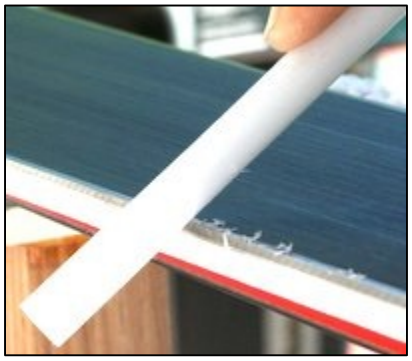

Figure 1: Ski Vision's Tuning Stick being scraped across an edge to test its sharpness

1.4. Approach

To satisfy the goal of creating a device to measure ski edge sharpness, our project divided into two areas of work: a research segment dedicated to determining the proper scale to measure the curvature of the edge and a design segment focused on developing a portable device based on the scale and curvature research. First, rectangular steel samples, each finished with different amounts of controlled wear, will be manufactured to simulate real ski edges. Next, each edge will be scanned under an Olympus LEXT OLS4100 microscope to measure the 3D surface. Curvature measurements are extracted at various scales using a calculation program developed by the WPI Surface Metrology Lab based on Heron's Method from calculus (Vulliez et al., 2014). Tests to measure the tangential friction of the simulated ski edges will be conducted with a friction testing device also developed by the WPI Surface Metrology Lab. The curvature and force data will be plotted to test for correlations and to identify an ideal scale range for measuring sharpness, quantified as curvature. The final step is designing a portable device to measure curvature at the ideal scale range.

2. Research

2.1. Introduction

Currently, there is no quantifiable way to define the sharpness of a ski edge. Qualitative tests show implied sharpness, however no method exists for knowing an exact geometric relation and how it relates to performance. Research was conducted to shrink this knowledge gap. Testing was conducted to measure geometric relation, the curvature, of an edge and see how different edge profiles performed under different tangential forces. This correlated data defined a scale range to measure for the ideal geometry for the forces applied.

2.1.1. Objective

The objective of this section of the Major Qualifying Project (MQP) is to find the optimal scale for measuring the curvature of a ski edge.

2.1.2. Rationale

Little quantifiable data is known about how ski edge sharpness relates to the ability of a skier to hold onto a path through a turn. A skier loses precious time in a race if they slip through a turn instead of holding a steady, slicing path. Intuitively, sharper edges seem like the better choice for holding throughout a turn, however equally intuitive, duller edges might be better in some snow conditions. Research needed to take place to give insight on how the geometry of a ski edge relates to edge performance.

2.1.3. State of the Art

Skiers tune their ski edges to reduce slippage and increase grip on snow and ice during a turn. Dozens of sharpening files, stones, and bevels are on the market that can be used to sharpen ski edges. Professional ski tuning (sharpening of the edges), currently an art, needs to become a science to advance the sport of ski racing. Current processes and products can be adapted for the intent of measuring the optimal sharpness of a ski edge.

2.1.3.1. Profile Extraction

Laser scanning confocal microscopes are used to measure the surface topography of an object. Applying this concept to measuring ski edge geometry, one can position a ski edge or a simulated one, at a 45 degree angle under a microscope to generate a symmetric surface measurement (Gleason et al., 2013). Software such as Mountains by DigitalSurf, then extracts a cross-sectional edge profile from this 3D measurement. This profile represents the geometry of an edge.

2.1.3.2. Curvature Calculation

Curvature, k_h, is the inverse of radius and changes as a function of the scale of observation (Vulliez et al., 2014). Heron's Method calculates the curvature as a function of scale on a profile. As seen in Figure 2, the formula fits a triangle to a profile by selecting three points at a specific scale. Scale is defined as the horizontal distance between the first and third point, the second point is selected at the middle distance. The area of the circumscribed triangle is then used to calculate the curvature. Curvature measurements can be extracted in CurvSoft from profiles generated in Mountains software (Gleason et al., 2013).

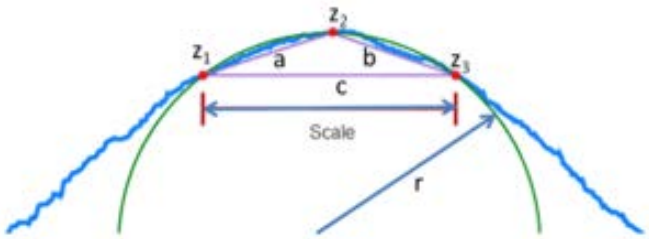

$$s = \frac{a+b+c}{2} \quad (1)$$

$$h = \sqrt{s(s-a)(s-b)(s-c)} \quad (2)$$

$$k_h = \frac{1}{r} = \frac{4h}{a*b*c} \quad (3)$$

Figure 2: Definition of profile points for curvature calculation. Adapted from (Gleason et al., 2013)

2.1.4. Approach

The goal of our research was to find the ideal scale for measuring curvature of a ski edge. We followed the process depicted in the graphic below:

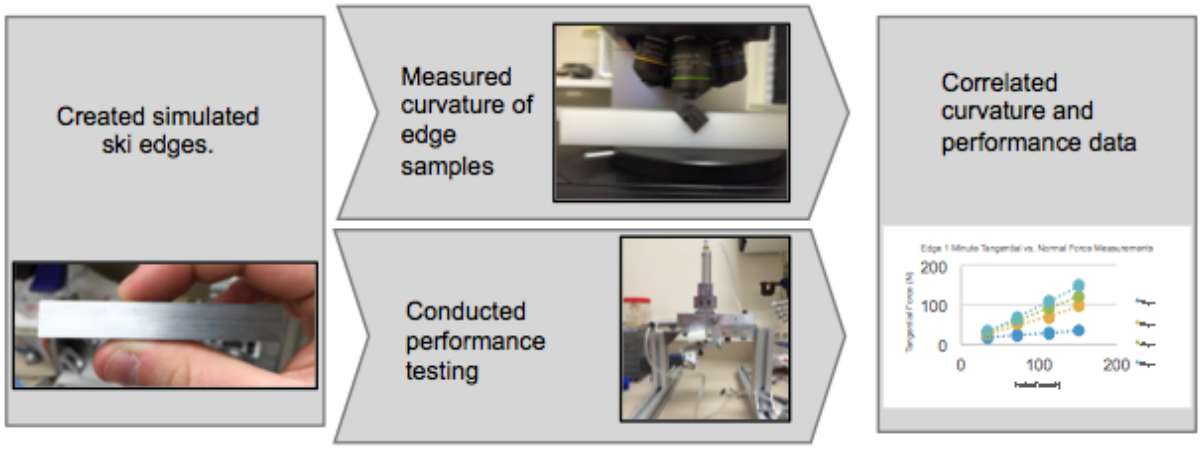

Synthetic edges were manufactured so we could have controlled edge samples. Measuring the surface of edge samples with a 3D confocal microscope took place next. Afterwards we extracted curvature and conducted performance testing simultaneously. To clarify, we are examining performance as a function of the cross-sectional profile as shown in Figure 3. Finally, the curvature measurements and performance testing results were plotted against each other in graphs to see if correlations between these two independent variables existed.

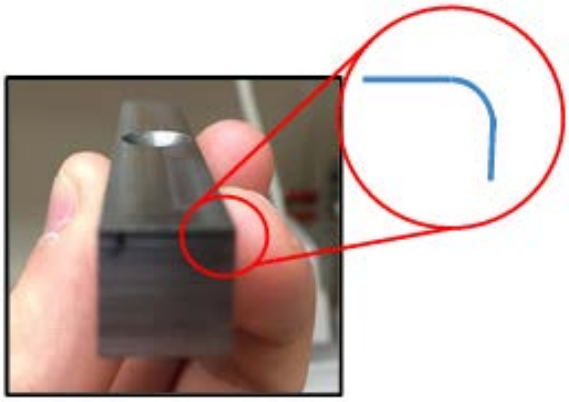

Figure 3: Edge Sample

2.2. Methods

2.2.1. Manufacturing

Because we did not have an easy way to measure actual skis edges with the 3D confocal microscope or test in our performance testing apparatus without cutting up a ski, we created rectangular metal edge samples to use instead. Adapting from the process of a previous WPI MQP (Burton et al., 2013), we manufactured and prepared edge samples to have similar characteristics of actual ski edges. Five identical edge samples were milled from 1045 steel. The edges were honed using a SKS rubber edge deburrer to remove the burr created by machining. Four edges were finished in a mass finisher for 1, 2, 4, and 8 minutes respectively to create controlled and varied wear. One was honed using traditional ski edge sharpening techniques as a comparison. The procedure in Appendix F outlines in detail how we created the simulated ski edges.

Figure 4: Edge undergoing milling operation

Figure 5: Edge sample being mass finished

2.2.2. Curvature Analysis

To produce 3D renderings of our edge samples we used the Olympus LEXT OLS4100 confocal laser-scanning microscope in the WPI Surface Metrology Lab. Edge samples are set up in the microscope at a 45 degree angle in line lengthwise with the y-axis. A 3D surface measurement of the edge is taken with the highest level of magnification. Once a 3D measurement file exists, the measurement is put through a filter that minimalizes the outlier data points, maximizing accuracy. A cross-sectional 2D profile of the 3D surface measurement is extracted using Mountains. The profile is then imported into CurvSoft, which calculates curvature at different scales along the profile of the edge. Data was exported in .csv file format that is then imported into Excel for further evaluation. For step-by-step instructions to conduct curvature analysis, please see Appendix I.

2.2.3. Testing and Data Acquisition

2.2.3.1. Tester

The testing device currently used in the WPI Surface Metrology Lab is the culmination of several years of design and modification. Today, the system uses two pneumatic cylinders actuated by two screw valves. On each cylinders' airline are two pressure gauges, one analog and the other digital. The two cylinders connect in normal and tangential positions to the frame of the testing apparatus. On the front and back of the tester's frame are clamps that hold a polyethylene block containing an edge sample. These adjust to have test angles of 30, 45, and 60 degrees. The test material resides in a cavity of the testing block on the underside of the normal force cylinder. Normal force is applied so the test material contacts the edge sample. Tangential force is applied to represent the grip strength of the edge.

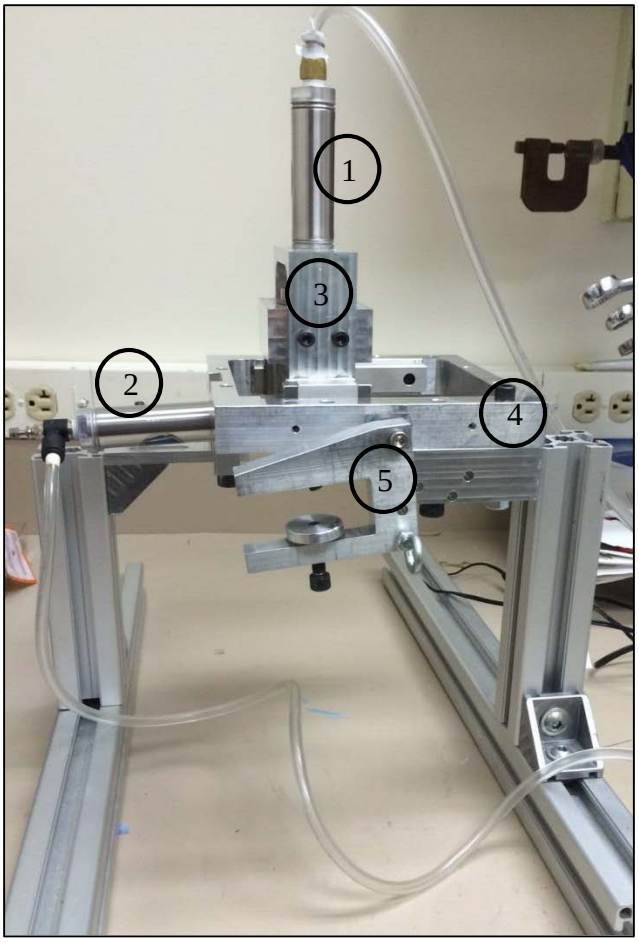

Figure 6: Tester Assembly (1) Normal Cylinder (2) Tangential Cylinder (3) Testing Block (4) Frame (5) Edge Holder

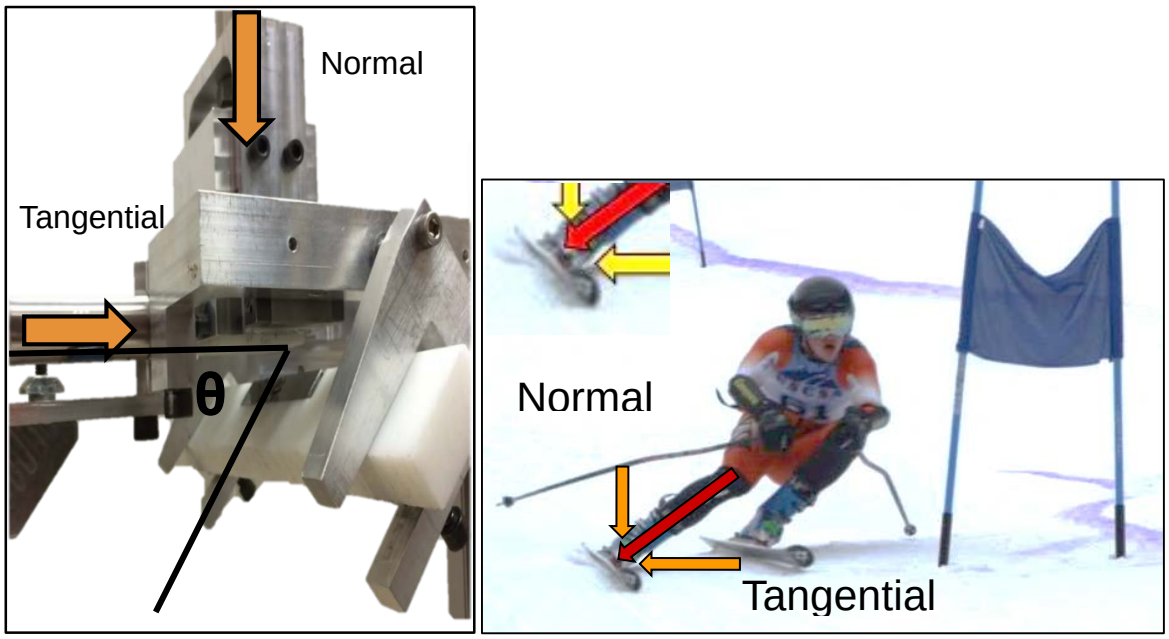

Figure 7: Tester and skier displaying tangential and normal forces

2.2.3.2. Testing Setup

To set up for testing, an air supply is attached to the cylinders. Then the edge sample is fixed to the polyethylene holding block and then the block is placed in the holding clamps. The holding clamps are set to the desired edge angle, 30, 45, or 60 degrees, using a pin through the concentric holes on the tester frame and the edge clamps. From there the testing material is loaded and locked into the cavity under the testing block

To set up the edge sample for a test, a small tangential pressure is applied to move the testing block up to the first line on the testing block rail. Then a small normal pressure is applied to gently bring the testing material down onto the edge sample. The way the edge holding block rests in the clamps is adjusted under this light normal pressure to ensure complete contact between the material and the length of the edge sample.

2.2.3.3. Testing Procedure

After the edge sample is secured and balanced in the testing apparatus, the testing procedure can begin. Typically the testing material is loaded into its square cavity at the bottom of the testing block and locked into place by tightening the tangential cylinder. Then the testing block is moved up to the first line on the testing rail by applying a small tangential pressure. With the block in place the desired normal force can be applied down onto the edge. This will create solid contact between the testing material and edge sample at the edge angle set in the testing setup. Tangential pressure is gradually applied until the edge sample slips across the testing material and moves down to the second reference line on the testing rail. The tangential pressure that causes the material to give way is recorded in correspondence with the normal force that was applied and the angle the edge sample was set to. After testing is completed, pressure can be released in both cylinders to bring the testing block back to home. The testing material can be removed and resurfaced and the procedure is repeated.

2.2.3.4. Testing Materials

Instead of using actual snow and ice, we used different plastics that were representative of different snow conditions and could be used extensively in our indoor testing facility.

Ultra-High-Molecular-Weight (UHMW) Polyethylene:

Polyethylene is a relatively rigid thermoplastic used to simulate hard packed, icy snow. During testing, the material deformed slightly under the normal force and sheared off in small flakes under the tangential force. The polyethylene blocks were resurfaced after each test using 120 grit sandpaper to smooth ridges formed during the previous test, then finished with 320 grit sandpaper. While sanding, the block was moved straight back and forth so the sandpaper would cut tiny striations in a single direction into the surface. These striations were set up perpendicular to the orientation of the edge during testing to make sure the striations had minimal effect on the friction test.

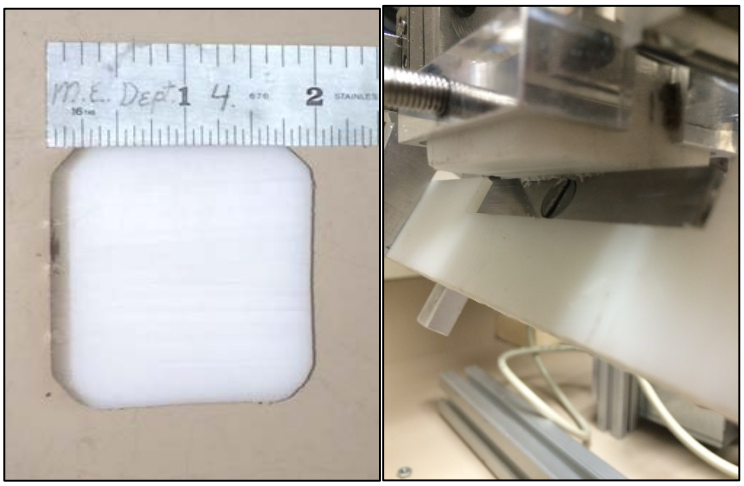

Figure 8: Polyethylene sample and in contact with edge

Machinable Wax:

Machinable Wax is a softer material than polyethylene used to simulate softer snow. This material deformed into thin chips instead of fine dust. The blocks were resurfaced using a short facing operation in a CNC mill after each test.

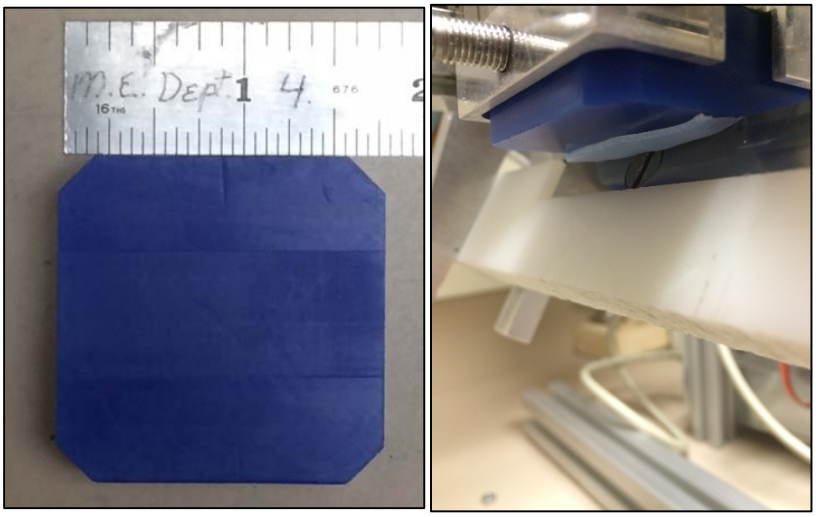

Figure 9: Machinable Wax sample and in contact with edge

Ice:

Molds made from machineable wax were created to make ice samples that could fit into the tester. The ice samples were brittle and sheared into a wet dust during testing. Testing of ice was limited due to the fragile and unpredictable nature of the samples and the lack of below freezing testing conditions.

Figure 10: Ice Sample

2.2.4. Data Analysis

2.2.4.1. Force Graphs

After performance testing with the test apparatus, the normal and tangential force data were input into Microsoft Excel. The data was separated by edge sample type (1, 2, 4, and 8 minutes in the mass finisher) and the edge angle of performance testing. Data was converted from psi to newtons. The spring forces for each piston were taken into account and subtracted from the converted forces to represent the actual forces applied to the edge sample. The normal force was plotted in the x – axis and the tangential force in the y – axis. This process was repeated for all of the edges, as this data was necessary for the next step in analysis.

2.2.4.2. Combining Force and Curvature Values

At this point, we had two independent sets of data, edge geometry quantified as curvature and performance data quantified as the x-coefficient of the trend line of the tangential versus normal force graphs. We plotted the x-coefficients against the curvature at distinct scales to see if the data would correlate. We grouped data by the edge angle of the performance tests, 15, 30, 45, and 60 degrees and by the scale of the curvature measurement. On these graphs we used an exponential trend line to generate an R^2 value. The R^2 values from these graphs were then plotted against the scale at which the curvature measurements were taken and grouped by edge angle. This left us with four graphs, one for each edge angle that represented the relationship between scale and curvature performance. Good correlations were considered to be R^2 values above 0.9 and excellent correlations were considered to be R^2 values above 0.95. For an in-depth depiction of correlating curvature and force data, please see Appendix I.

2.3. Results

2.3.1. Performance Graphs

Strong correlations were found between the normal and tangential forces. The relationship was validated by having R^2 values greater than 0.95 on all graphs. These graphs showed that the tangential forces causing the edge to slip increased with increase normal forces and increased edge angle. Figure 11 demonstrates this relationship. The results with polyethylene showed that the sharper the edge, the higher the tangential force is required for the edge to slip. However, preliminary results for machinable wax showed in some cases duller edges required a greater tangential force to cause the edge to slip. All performance graphs can be found in Appendix G.

In order to get a better correlation in our force versus curvature graphs, we removed the honed edge data. Correlations jumped from 0.7 to above 0.9 in R^2 values. We justified this removal because the honed edge was not mass finished and therefore would have a harder time correlating with the data.

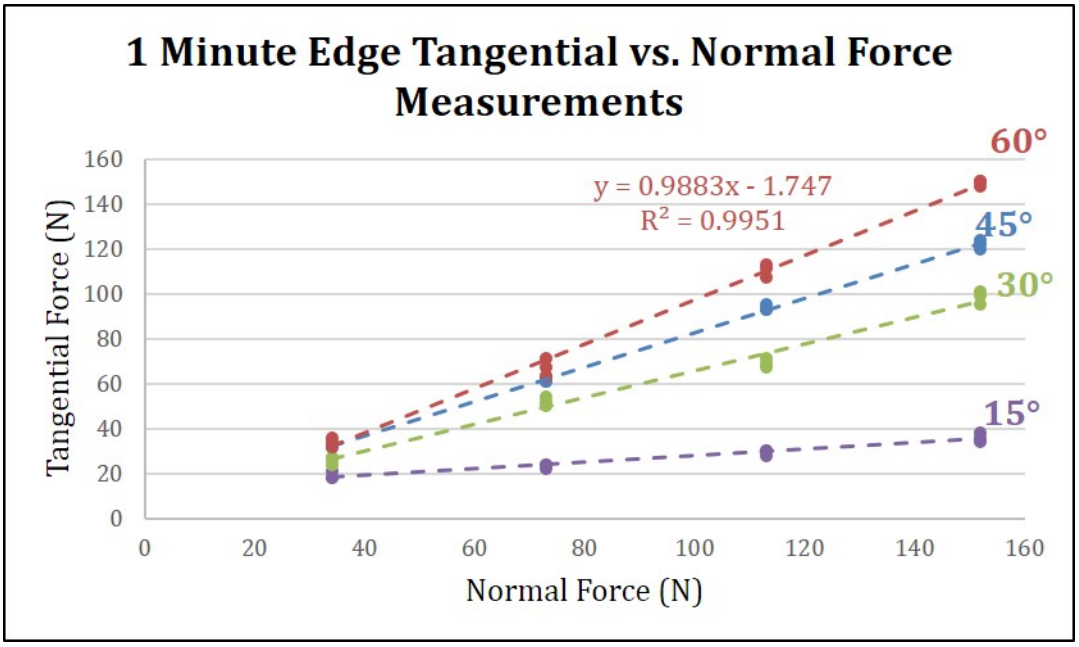

Figure 11: Tangential vs. Normal Force graph for 1 minute edge

2.3.2. X-Coefficients vs. Curvature Value Graph

To make correlations between the performance graphs and curvature measurements, the slope of the linear trendlines in the performance graphs were plotted against the absolute value of the edge sample's curvatures measured at specific scales. Using an exponential trendline, we found that there were multiple scales for the 30, 45, and 60 degree angles which attained R^2 values around 0.9. However, the 15 degree data did not show strong correlations. Figure 12 shows an example of a T/N vs. curvature plot that was made. More plots can be found in Appendix H.

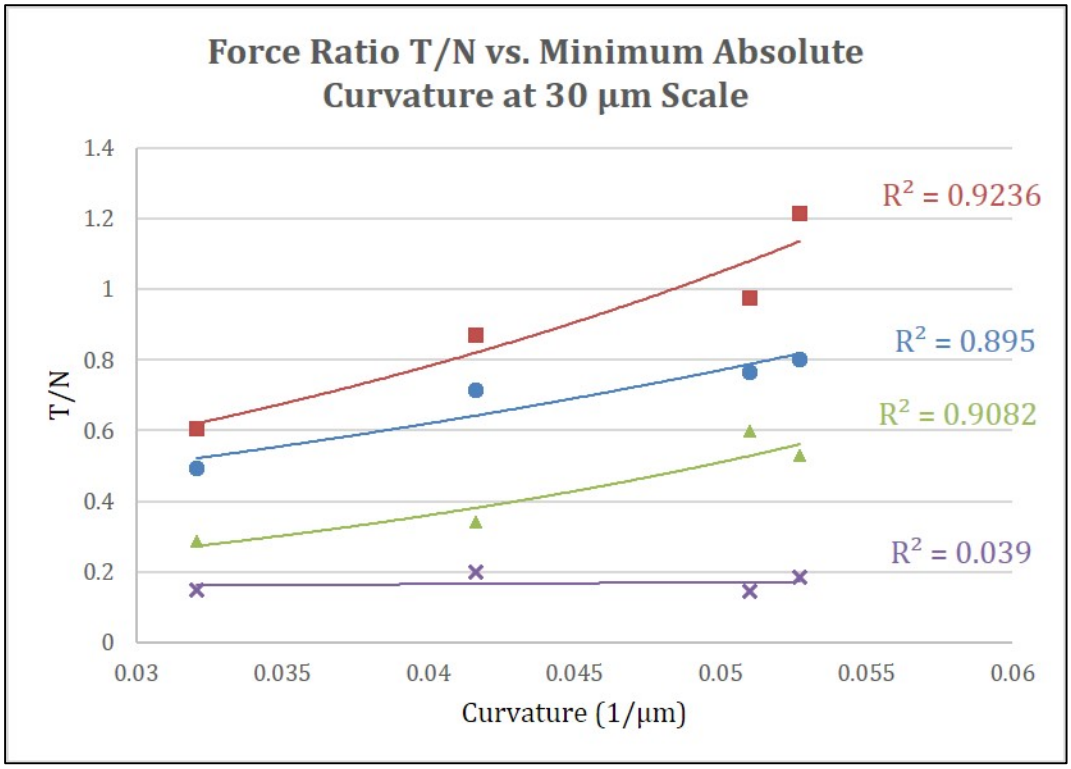

Figure 12: Curvature correlations for each angle

2.3.3. Graphing R^2 vs. Scale

After the Force Ratio vs. Minimum Absolute Curvatures were plotted, the R^2 for each scale and angle were plotted versus the scale at which the curvature was calculated. Figure 13 shows this correlation. For 45 and 60 degrees, there are multiple scales that have strong correlation ($R^2 > 0.9$). Additionally, there are also some scales with strong correlations for 30 degrees. No strong correlations were found for 15 degrees. The range of scales at which the graphs had the strongest correlation with the 30, 45, and 60 degree angles were between 30 and 50 µm.

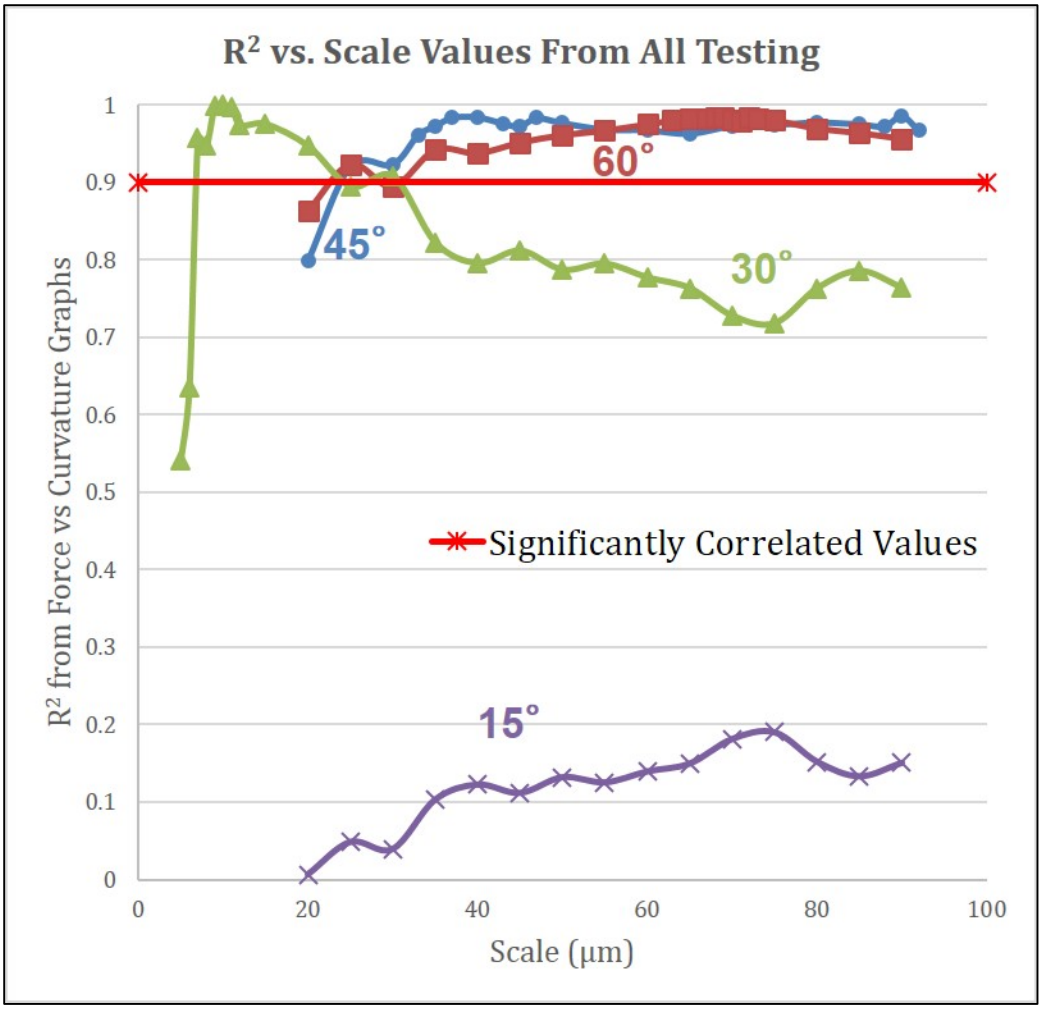

Figure 13: Correlations of curvatures at each scale

2.4. Discussion

2.4.1. Edge Preparation Procedure

When creating the simulated edges, we tried to prepare the edge samples as efficiently as possible. One method for reducing cycle time was to design a pair of soft jaws to hold the edge samples. This allowed the three edges to be faced off in one operation, however this fixture could have been better utilized if the edges samples were cut to a more consistent length.

Figure 14: Soft jaws fixture

Another important component was removing the burr formed during machining. During testing where burrs were present, weak correlations were found between the normal and tangential forces. Upon reviewing the Olympus LEXT OLS4100 Microscope renderings, it was observed that there was clearly a burr present on the edge, as shown in Figure 15.

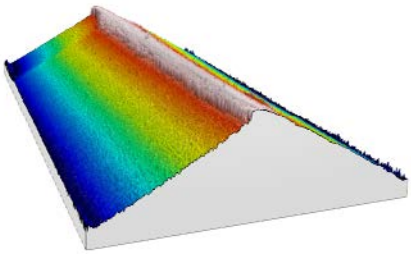

Figure 15: Edge with burr present

When the next set of edge testing was conducted, we used a SKS rubber edge deburrer (no. 3246) as part of the finishing process to remove the burr from the edge samples. The LEXT Microscope was used to verify that the burrs had been removed from the edge samples after machining. After implementing burr removal, all four edge samples went into the mass finisher to be rounded. The edge samples then showed strong correlations between tangential and normal forces. Figure 16 shows that the burr was successfully removed by using a SKS rubber edge deburrer.

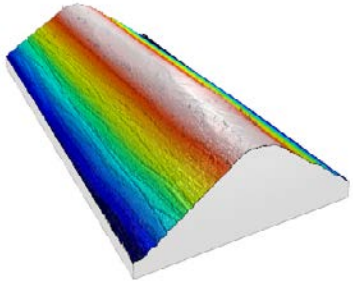

Figure 16: Edge with burr removed

When comparing the burr versus deburred datasets the edges with burrs had higher slope values in the tangential force vs. normal force graphs. A burr present on the edge required a

greater tangential force for the edge to slip than without a burr. This data makes sense because the burr would catch on the polyethylene, requiring a greater force for the edge to slip. Removing the burr on the edges provides a more realistic dataset because it provides a better representation how skis are actually tuned.

2.4.3. Limitations and Critiques

Many of our conclusions are based on using polyethylene as our snow sample. Further testing should be conducted with different snow simulation materials. A database of ideal curvature values with associated snow conditions could be stored in a measuring device, allowing ski tuners to select the proper curvature to tune their skis.

Although machinable wax was also used as a snow sample to conduct friction tests, the edge samples were not refinished before tests were conducted. There were noticeable deformations to the edge after polyethylene testing, shown on the microscope. Refinishing the edges after conducting polyethylene testing could have produced different results. A protocol should be established for refinishing edges after a certain number of tests or when testing with a new material begins.

2.4.3.1. Repeatability of Testing with Ice

Testing with ice was conducted outdoors in late February when the ambient temperature was 15 degrees Fahrenheit. Ice samples were made to fit in the tester using machinable wax molds. Out of the six samples that were produced, only four could be used in the tester. During testing, the same edge sample and normal force were applied, each instance resulting in different tangential forces. The surfaces and consistency of ice samples are too variable to produce repeatable results with the current tester design. If future testing with ice is desired, the design of the tester needs to be reworked to accommodate the ice. Making ice samples in the sacrificial molds made it difficult and expensive to produce a small amount of samples that did not perform well.

2.4.4. Representing the Performance Data

While experimenting to find correlations in our performance data versus curvature, we tried three methods to represent the force component. We attempted using the ratio of tangential versus normal for each individual test, the same ratio averaged across tests, and then finally the x-coefficient for the tangential versus normal graphs. The x-coefficient was most effective because it was an average of all the data points. This helped to normalize the outlier points as well as provide a more consistent data point to use for correlations.

2.4.5. Testing Modifications

2.4.5.1. Peg Board

When we first started working with the edge tester, it was difficult to produce repeatable results. The angle of the edge holders had to be individually measured and tightened down, leaving room for variability in the edge angle. To solve this problem, we designed attachments for the frame of the tester with a series of holes. These holes are concentric with the holes on the edge holders. When the edge holders are oriented at angles of 30, 45, and 60 degrees, a pin can be inserted through the two concentric holes to set the holders at fixed angles.

Figure 17: Peg holes used to set edge angles

2.4.5.2. Addition of Digital Gauges

Towards the end of our project timeline, a set of digital gauges were added to the airlines of both the tangential and normal cylinders. These new gauges measure pressure with greater resolution and monitored small changes more easily. The digital gauges were used instead of the analog gauges for collecting the machinable wax data. However, the pressure on the digital gauges read in psia versus the analog gauges, which read in psig. This difference in the units for pressure was factored using a simple conversion.

2.4.5.3. Factoring Spring Forces

Starting with the second round of testing with polyethylene, the spring forces of the pistons were factored into the performance data. It was determined that the normal force piston had a retracting spring force of 25 newtons while the tangential force piston had a retracting spring force of 27 newtons. Although the force values were adjusted for the spring forces of the pistons, the slopes of the tangential vs. normal force graphs did not change. Only the y-intercepts shifted proportionately because these performance values are linear.

2.5. Conclusions

1. Tangential force required to cause slip increases with increased edge angle
2. Results indicated that edges should be finished to different curvatures for different material conditions
3. R^2 correlations between curvature and performance improve as edge angle increases
4. Optimal correlation between curvature and performance was found in the scale range of 50 – 70 µm for data relating to edge angles of 45 and 60 degrees.
5. Optimal correlation for edge angles of 30, 45, and 60 was found in the scale range of 20-30 µm.

Based on all of the performance testing, results indicated that edges should be finished to different curvatures for different material conditions, For example, duller edges held better than the sharper edges in the softer machinable wax and sharper edges held better on the harder polyethylene. Although this might seem initially counterintuitive, it can be explained. On harder material, a sharper edge can dig into and hold onto a material. A duller edge is more likely to lose grip and slide on a hard material. On softer materials, it is easier for a sharper edge to slice through the material, meaning it will slip under less force. Alternatively, a duller edge cannot move as easily and will hold better. More testing with different materials should be conducted to get a better understanding of this phenomenon. From the current results, it is observed that there might be an optimal edge sharpness for different materials.

Upon inspecting the scale of curvature versus the R^2 value graphs, correlations improve as edge angle increases. The majority of 45 and 60 degree R^2 data reside above a value of 0.9. The 15 degree R^2 data hovers around 0.2. This data suggests that as more of the edge profile was engaged in the material, the more the geometry played a part in how well an edge held under performance testing.

Another observation from the scale versus R^2 graphs indicates an optimal curvature range for ski edges. Most of the 45 and 60 degree R^2 values above 0.9 were found in the scale range between 50-70 μm. We focused on the 45 and 60 degree results as these angles directly compared to ones an actual ski racer encounters while turning. After confirming optimal performance correlation at this scale range, we now have the best range of scale for observing the relationship between curvature and performance.

2.6. Limitations

2.6.1. Method to Resurface Machinable Wax

Although machinable wax was able to produce consistent and repeatable results, resurfacing the machinable wax samples required significantly more time than polyethylene. Because a chip was formed in the machinable wax, resurfacing was required after every test. Each machinable wax sample had to be faced off using an endmill on a milling machine. The entire resurfacing process took approximately 2 - 2.5 hours for 6 samples that could only produce 12 tests. A heating element, such as a ski waxing iron, could be used with greater efficiency to resurface the machinable wax similar to how a Zamboni is used to resurface ice. Designing a fixture, capable of holding multiple machinable wax samples in a vice jaw such that the mill offsets only had to be set once would eliminate the need to change work offsets each time.

2.6.2. More Tests with Machinable Wax

Significantly less data was produced for machinable wax than for polyethylene. This was in large part due to the longer preparation time of machinable wax as well as the need to reface each block after conducting performance testing on the two faces of the blocks. Additionally, the use of machinable wax was introduced later within the project timeline, limiting the amount of available testing time. In order to better understand the correlations that were presented as well as validate the data overall, more testing with machinable wax should be conducted.

2.6.3. Resurface Edge Samples

More accurate performance data for each edge could be generated with an increased number of tests. During our tests, each edge underwent a total of 48 tests before being reimaged and remachined. The time required to machine 5 edge samples is about 4 – 5 hours, which makes remachining an unrealistic operation after each test with the current process. During our manufacturing, we only deburred one edge of an edge sample, which prevented us from conducted test with the other three edges. Instead, deburring of all four edges of an edge sample before mass finishing could be one way to generate more tests.

2.6.4. Longitudinal Testing

Considering that ski edges experience tangential and longitudinal forces during use, performance testing for both was attempted. However, the acquisition of longitudinal performance data was not feasible with the current design of the performance tester. The same process of incrementally increasing the normal force was used as tangential performance testing. The tangential force cylinder was set in line with the edge. Even with the largest normal force being applied onto the edge, the slightest longitudinal force caused the edge to slip. As a result no conclusive data was collected from the longitudinal performance testing.

2.6.5. Redesign Tester for Robustness and Repeatability

The current performance tester design is good at producing repeatable results but only performing a long testing procedure for each friction test. The tester is not robust and requires a considerable amount of testing time being spent making sure that it is working correctly. Often the airlines sprung leaks at the connection points or the joints of the tester needed to be adjusted so the testing block could move correctly. The way the material sample is loaded into the tester is also extremely inefficient and requires using one of the air cylinders as a fastener when the cylinder should have its own dedicated fastener.

If more friction testing were to continue, the design of the tester needs to be re-evaluated to make testing more streamlined and precise. The performance tester should be configured in a way that the components cannot be easily influenced by the large forces they undergo during testing. Much of the current testing procedure is dedicated to getting all of the different components in place to actually perform the test. Reducing the time between tests is critical for producing large amounts of data. An easier way to load the sample material and fixture it without having to move the position of the tangential cylinder would also make testing more repeatable. Above all, the airlines and valves used to operate the pneumatic cylinders need to be either redone or reconfigured to reduce potential for air leaks.

2.6.6. A more precise method to determine optimal radius over a range of materials

From our research, we were able to approximate an ideal radius for a ski edge in certain conditions. We conducted our research to find the ideal scale at which to read curvature and found for edges that were being applied at 45 or 60 degrees, that a scale range of around 70 μm was ideal. Knowing the ideal scale, we then backtracked and went back to the force versus curvature graphs at this scale. Because we used all four edge curvature values, there was a range of curvature at which the best correlation of force was taken. Knowing that curvature is the inverse of radius, we were able to take the inverse of the extremes of the curvature range in order to output a range of radius values. This implies that there could be an ideal radius for different snow conditions. This also poses the question of our process robustness; could it improve with better sharpening techniques? Furthermore, this radius range does not factor in the effect of tangential forces. We are unsure how we would factor tangential edge loading into the ideal radius conclusion, but additional testing might conclude that this might affect the ideal measurement scale.

2.7. References

2015 SIA Snow Sports Fact Sheet. (2015, January 1). Retrieved April 26, 2015, from http://www.snowsports.org/Retailers/Research/SnowSportsFactSheet

Bruton, F. D. S. a. M. E., Close, J. E. S. a. M. E., Hopkins, J. M. S. a. M. E., Dragonas, M. J. S. a. M. E., & Brown, C. A. F. a. M. E. (2013). Measuring the Quality of Ski Edges. Worcester, MA U6 - ctx_ver=Z39.88-2004&ctx_enc=info%3Aofi%2Fenc%3AUTF-8&rfr_id=info:sid/summon.serialssolutions.com&rft_val_fmt=info:ofi/fmt:kev:mtx:book&rft.genre=book&rft.title=Measuring+the+Quality+of+Ski+Edges&rft.au=Hopkins%2C+Jason+Matthew+Student+author+--+ME&rft.au=Dragonas%2C+Michael+Joseph+Student+author+--+ME&rft.au=Close%2C+Jocelyn+Elizabeth+Student+author+--+ME&rft.au=Bruton%2C+Frank+Daniel+Student+author+--+ME&rft.date=2013-01-01&rft.pub=Worcester+Polytechnic+Institute&rft.externalDocID=1849592&paramdict=en-US U7 - eBook U8 - FETCH-wpi_catalog_18495923: Worcester Polytechnic Institute.

Gleason, K, Lemoine and Brown. (2013). Profile Curvatures by Heron's Formula as a Function of Scale and Position on an Edge Rounded by Mass Finishing.
Materials, A. (2014). Creating 3D Ski Edge Measurements Using OLYMPUS LEXTOLS4000. Retrieved 11/4, 2014, from http://www.azom.com/article.aspx?ArticleID=11191
Sewell, M. All About the Tuning Stick: SkiVisions, Inc. Retrieved 11/4, 2014, from http://skivisions.us/1693.html
Vulliez, M., Gleason, M. A., Souto-Lebel, A., Quinsat, Y., Lartigue, C., Kordell, S. P., . . . Brown, C. A. (2014). Multi-scale Curvature Analysis and Correlations with the Fatigue Limit on Steel Surfaces after Milling. *Procedia CIRP, 13*, 308-313.

3. Design

3.1. Introduction

Tuning is an essential part of ski racing but many racers sharpen their edges without actually knowing how sharp their skis are. Current sharpness testing methods are only good for measuring relative sharpness. Currently there are no devices on the market that can quantify the sharpness of a ski edge. Our team conducted static force testing to find a correlation between edge performance and curvature at a specific scale. This research assisted in the development of a portable device for measuring the curvature of a ski edge at incremental points along the length of a ski.

3.1.1. Objective

The objective of this section of the Major Qualifying Project (MQP) is to design a portable device that will be able to measure the sharpness of a ski edge by measuring the curvature of the edge at incremental points down the length of the ski.

3.1.2. Rationale

There is no quantifiable way to measure the sharpness of a ski edge. According to SnowSports Industries America, there are an estimated 16,343,000 alpine skiers and snowboarders in the United States (*2015 SIA Snow Sports Fact Sheet*, 2015). From avid tuners and ski racers to retail shops and manufacturers, this device could be integrated as a quality check into a preexisting tuning regimen. This device could also be beneficial in mitigating risk of injury by allowing the user be able to identify when their skis need to be sharpened. 2D laser scanning profilers currently exist for industrial applications, but few of these devices are portable and support the scale of measurement required to effectively measure ski edge curvature.

3.1.3. State of the Art

3.1.3.1. Laser Triangulation

The pairing of an optical line projection and a camera can be used to measure 3D shapes using a principle called laser triangulation, or sheet-of-light range imaging (Kumar et al., 2006). As shown in Figure 18, triangulation is achieved through the angles made by the camera, line projection, and the baseline length between the light source and the camera. When the line laser is projected onto a flat surface and viewed at an angle, there is no apparent distortion to the line. When the line is projected over a surface of varying 3D heights, the line shape will appear distorted in shape when viewed from an offset angle. The dislocation of pixels on this distorted line is directly related to the object's shape and can be used to optically triangulate the shape. Based on relating the dislocation of points to the triangulation in Figure 18, the object height at the measured can be defined as:

$$Object\ Height = \frac{B * s * \sec^2(\alpha)}{b_0 + s * \tan(\alpha)}$$

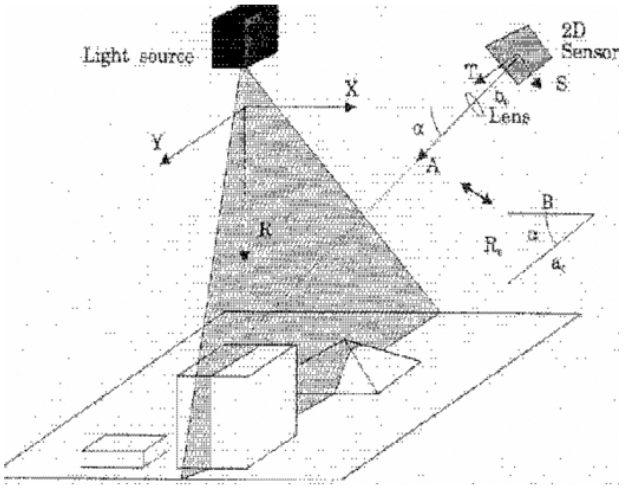

Figure 18: Laser Triangulation between light source, optical sensor, and distorted points on line (Kumar et al., 2006).

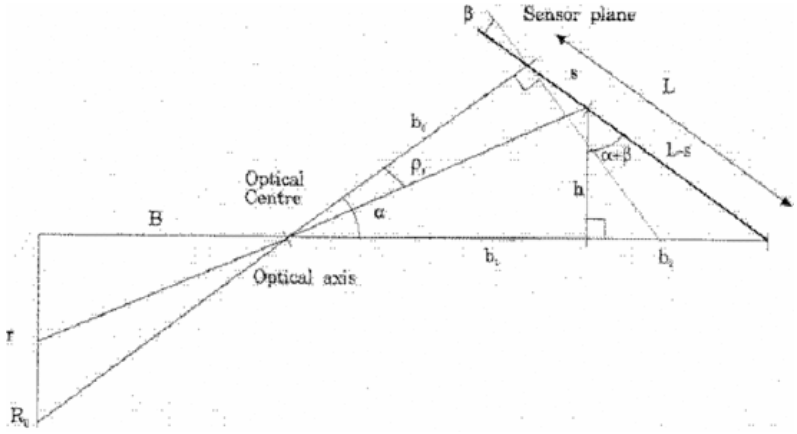

Figure 19: Triangulation for measuring object height (Kumar et al., 2006).

3.1.3.2. Image Processing

Image post processing is required following image acquisition. This is necessary to filter out the image background and isolate the laser profile for analysis. There are two notable methods for extracting a laser profile. The first method filters out pixels nonconforming to established maximum and minimum pixel intensity threshold values, which are associated with the center of the laser line (Kumar et al., 2006). The second method establishes minimum and maximum threshold values to divide the image into three categories: foreground, background, and undecided area. After the background is filtered out, an algorithm calculates a first point of the laser line and local line direction within the foreground of the image. The resulting points are then fitted with a smooth curve by a second algorithm (Chen, 2013). With the line profile extracted, CurvSoft can use the extracted profile to calculate curvature (Gleason et al., 2013).

3.1.3.2.1. iPhone Microscope Conversion

Researchers at the University of California developed an attachment system capable of converting a commercial smart phone into a microscope with roughly 175X magnification. By positioning a 1 mm diameter ball lens in front of a cellphone camera, the group was able to

produce images with a resolution of 1.5 μm in a 150 x 150 μm usable field of view before digital post processing. Resolution of the system was determined from using a 1951 USAF resolution target. While the usable field of view was limited due to flat field distortions caused by the spherical shape of the lens, image post processing techniques in MATLAB proved successful in increasing the usable field of view to 350 x 350 μm (Smith et al., 2011).

3.1.3.3. Relatable Patents

There are several companies, including Keyence Corporation, MTI Instruments, and Acuity that sell 2D laser scanner profilometers for industrial applications. Each of these companies has developed their own laser scanning profile sensor and compatible analysis software necessary for conducting measurements such as profile extraction. These companies most likely use their own variation of the technology described in US Patent 20090205088, which describes the application of optical triangulation to measure the profile of a 3D shape. This patent, *Optical Scanning Probe,* describes an optical profiler that captures several data points on the surface of an object through use of a light stripe projection and an imaging system capable of detecting light reflected off the object (Crampton et al., 2009).

Additionally, previous student projects and patents have been dedicated to determining quantifiable data about edges. One such patent, US7570369 B2, focuses on determining the size and shape of a machined piece by scattering radiation over the edge, collecting the reflected light, and then recording a picture of the edge geometry (Henrikson, 2009).

General Scanning Inc. is the original assignee of US Patent 5654800 that describes a triangulation based 3D imaging and processing method. This is conducted by associating height data with pixel intensity data of a laser light projected onto a measured object. This data pairing is then processed by a series of algorithms to convert the intensity values into greyscale and transmit the data set for processing by an image-processing computer (Svetkoff et al., 1997). Our device will use a similar method to generate height-pixel intensity data sets, which can then be imported into CurvSoft for curvature calculation.

A portable microscope system, the Proscope Mobile, has been produced under US Patent 20150029120. This patent describes a wireless microscope system that connects with a mobile user device such as a smart phone or tablet. The microscope is a handheld device that the user points at the desired object. Through an onboard wireless radio interface the user can control the microscope, capture images, store data, and transmit data all from a nearby mobile user device (Sieckmann, 2015).

3.1.4. Approach

The design segment of the project focused on developing a portable device that can characterize the sharpness of a ski edge. Because curvature changes as a function of scale, the research section established a range of optimal scales that best correlated to edge holding. This research identified the scale of resolution necessary for designing a measurement system. A benchtop model was developed to test the feasibility of an optical triangulation system that incorporated an iPhone as the camera system. Images of a line stripe projected onto an edge were captured and post processed in MATLAB to extract a profile of the edge for curvature calculation. This design will accomplish our objective by integrating ski holding performance data with preexisting optical triangulation methods to allow a user to assess the effectiveness of a tuning job.

3.2. Design Decomposition and Constraints

The device was developed using the principles of axiomatic design and is defined by our performance testing research. These functional requirements were designed to comply with the two axioms of maximizing independence and minimizing information content. Our design decomposition is laid out in Figure 20.

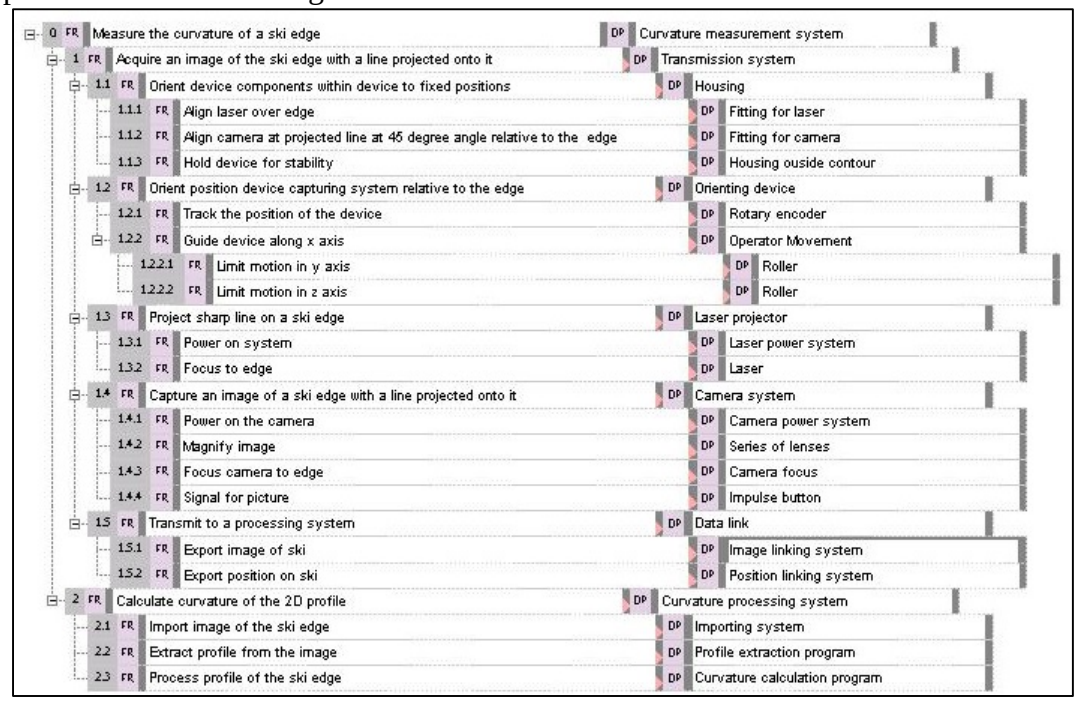

Figure 20: Design Decomposition

3.2.1. FR 0: Measure the curvature of a ski edge

At its highest level, FR0, the axiomatic design decomposition states the device must measure the curvature of a ski edge. This can be seen as the main function of the design and ultimately what the decomposition is trying to accomplish. This is decomposed into two parts, FR1 and FR2, which are children of FR0. These sum up to FR0 to measure ski edge curvature. DP0 is “Curvature Measurement System”, directly correlating to FR0.

3.2.2. FR 1: Acquire an image of the ski with a line projected onto it

FR1 states the device needs to acquire an image of the ski edge with a laser line projected onto it. DP1 is “Transmission System”. The theme behind this functional requirement is to assemble components appropriately in order to acquire images along the length of the ski suitable for calculating ski edge curvature.

3.2.2.1. FR 1.1: Orient device components within device to fixed positions

FR 1.1 was the need for a housing to secure all of the components. DP1.1 is “Housing” and represents fixturing the components through the use of another rigid body. The housing fixtures are important for securing components at predetermined distances and angles from each other and the edge to implement triangulation.

3.2.2.1.1. FR 1.1.1: Align laser over edge

A laser line must be projected onto the edge, perpendicular to the edge length to measure it. The laser will be oriented to the edge by fixturing through the housing, as evidenced by DP1.1.1 “Fitting for laser**”.**

3.2.2.1.2. FR 1.1.2: Align camera at projected line at 45 degree angle relative to the edge

Similar to FR1.1.1, FR1.1.2 aligns the camera relative to the edge. The camera is aligned at an established angle to the laser, used to calculate the edge height from pixel distortion.

3.2.2.1.3. FR 1.1.3: Hold device for stability

In order for the user to slide the device along the length of the edge, a feature must be added. DP1.1.3 is “Housing outside contour”. The contours added to the outside of the housing allow the device to be ergonomic and intuitive to use.

3.2.2.2. FR 1.2: Orient position device capturing system relative to the edge

Device movement must be constrained to pure linear movement to follow the length of the edge. Position tracking of the device on the edge also needs to be satisfied for relating sharpness to position along the length of the ski. FR1.2 accomplishes these parameters through its children. DP1.2 is simply “Orienting Device”.

3.2.2.2.1. FR 1.2.1: Track the position of the device

FR 1.2.1 tracks the device's position to correlate curvature to position along the length of the edge. This ensures that the user can tune the appropriate position on the edge. DP1.2.1 is “Rotary encoder”, a component that correlates wheel rotations to displacement along the edge as the device is moved.

3.2.2.2.2. FR 1.2.2: Guide device along x-axis

To maintain pure linear movement along the length of the edge, defined as the x-axis, a component is needed to constrain movement. DP1.2.2, “Operator Movement”, states that the device will be moved down the length of the ski by the operator.

3.2.2.2.2.1. FR 1.2.2.1: Limit motion in y-axis

To maintain movement only along the x-axis, movement along the y-axis must be constrained. This can be done with rollers oriented to constrain y-axis movement while still allowing x-axis movement.

3.2.2.2.2.2. FR 1.2.2.2: Limit motion in z-axis

To maintain movement only along the x-axis, movement along the z-axis must be constrained. This can be done with rollers oriented to constrain z-axis movement while still allowing x-axis movement.

3.2.2.3. FR 1.3: Project sharp line on a ski edge

A line projection is needed for profile extraction in post processing. DP1.3, “Laser Projector”, implies that a laser will be used to project a line onto the edge.

3.2.2.3.1. FR 1.3.1: Power on system

The laser must have a power source. DP1.3.1, “Laser power system”, powers the laser.

3.2.2.3.2. FR 1.3.2: Focus to edge

The laser must be focused to the edge for measurements to be taken. DP 1.3.2, “Laser”, states that a focusable laser will be used.

3.2.2.4. FR 1.4: Capture an image of a ski edge with a line projected onto it

The line projection needs to be captured in an image before a profile can be extracted. DP1.4 “Camera system” states that a camera will capture an image of the line projection. This camera system must have enough magnification and resolution to capture measurements within the scale range of 50-70 μm.

3.2.2.4.1. FR 1.4.1: Power on the camera

The camera must have a power source. DP 1.4.1, “Camera power system”, powers the camera.

3.2.2.4.2. FR 1.4.2: Magnify image

To capture an image of the edge capable of calculating curvature as a function of performance, magnification is required to measure at a scale of 50-70 μm. DP 1.4.2, “Series of lenses”, provides the camera with enough magnification to acquire the image at the required scale.

3.2.2.4.3. FR 1.4.3: Focus camera to edge

Fine adjustment might be needed to focus the camera system onto the edge. DP 1.4.3, “Camera focus”, allows the camera system to focus to the edge.

3.2.2.4.4. FR 1.4.4: Signal for picture

The camera system must be prompted to take the photograph of the edge. DP 1.4.4, “Impulse button”, signals the camera to capture an image.

3.2.2.5. FR 1.5: Transmit or link to a processing system

Post processing of the image is required to generate a profile of the edge. DP1.5, “Data link”, exports the height and position data associated with the image.

3.2.2.5.1. FR 1.5.1: Export image of ski

The image needs to be exported to processing computer for post processing. DP1.5.1, “Image linking system”, moves the image from the device's camera to the processor.

3.2.2.5.2. FR 1.5.2: Export position on ski

The position needs to be exported to processing computer for post processing. DP1.5.2, “Position linking system”, moves the position of the image from the device's tracking system to the processor.

3.2.3. FR 2: Calculate curvature of the 2D profile

The post-processing computer receives the image and position data from the device, extracts the profile from the image, and calculates the curvature of that profile. The resulting curvature is presented to the user.

3.3. Physical Integration

The physical integration of these aspects into a 3D CAD model, shown in Figure 21, provides a visual interpretation of the system and a platform for prototyping.

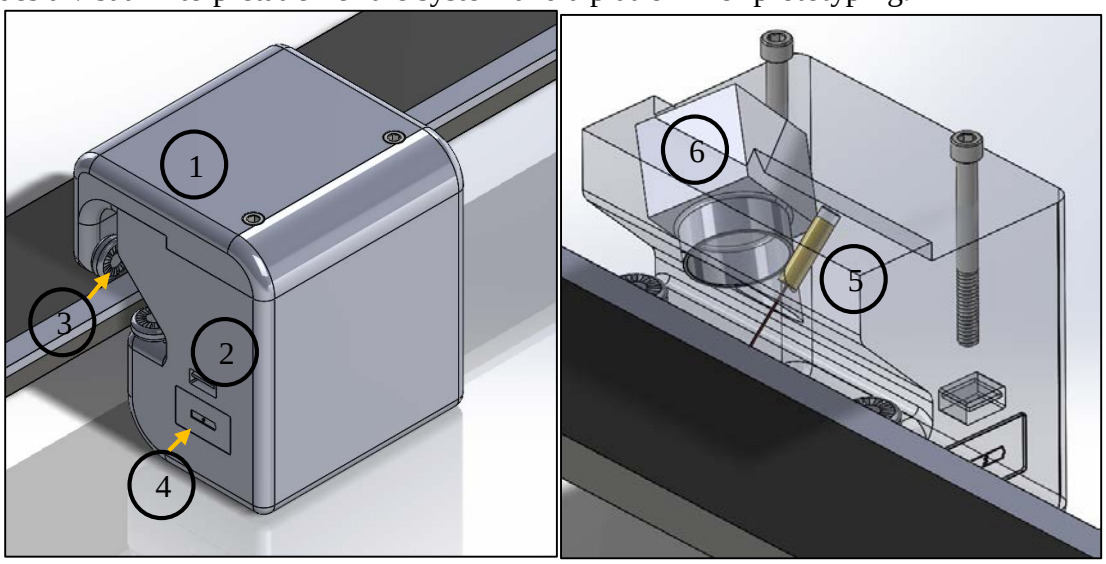

Figure 21: Design solid model

The first functional requirement incorporates the housing. The housing positions the components within the device. In this particular case, the laser and camera components will be fixed. To accommodate for this, the housing will be manufactured with openings in which the laser and CCD camera will be placed and held. This is represented in the solid model as component 1.

To accommodate for device manufacturability, the device needed to both be small enough to maintain its portability and also minimize assembly. The solid model has the housing divided into two main parts. These two pieces could be 3D printed, which is suitable for prototyping. Aside from fixturing the laser and the CCD camera, the housing is also responsible for holding internal electrical components. These include the USB drive for data transfer, rotary encoder to track position, and power supply for device power. These components are represented as 2, 3, and 4, respectively in Figure 21.

DP 1.2 incorporates a position device capturing system relative to the edge, divided into two components. First the device has to maintain motion along the x-axis, define in Figure 22, which is the direction along the length of the ski. This allows for the device components to remain correctly positioned relative to the edge. This is accomplished through two sets of rollers: one oriented to run along the base of the ski while the other oriented to roll along the sidewall. This system prevents contact with the edge while maintaining pure linear movement along the x – axis.

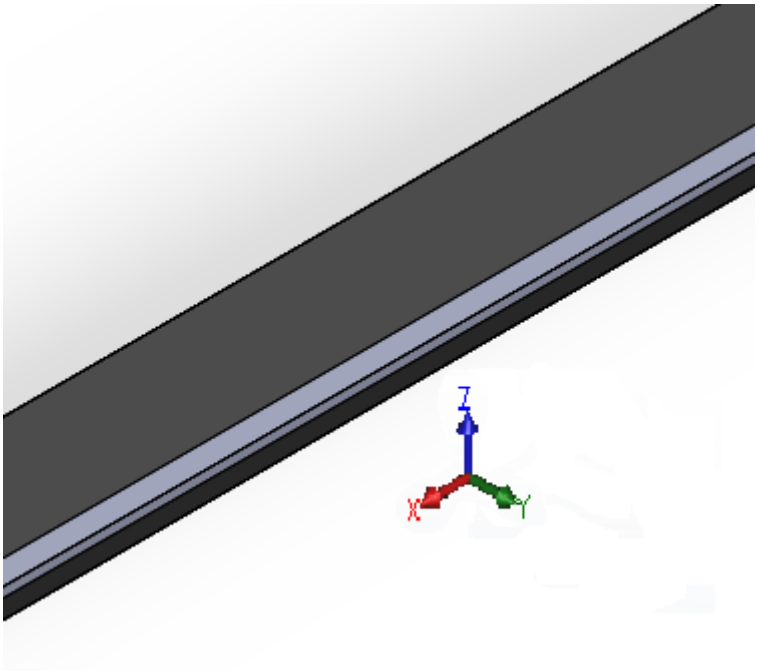

Figure 22: Coordinate axis of ski

To track the device's position along the length of the edge a rotary encoder was implemented. Note that the rotary encoder is represented by wheels marked 3 in Figure 21.

DP 1.3 projects a laser line onto the ski edge and is used to define the edge's profile. By projecting this line onto the edge, the device can extract a profile of the edge with the aid of post-processing. The line laser is denoted as component 5 in Figure 21.

DP 1.4 captures an image of the ski edge with the laser line projected onto it. In order calculate curvature with CurvSoft, a profile of the edge with associated height values is required. This can be extracted from an image of the laser line projected onto the edge. The CCD camera

must be powered on and signaled to capture an image. The image taken will need to be exported for post processing. From our benchtop testing, we determined that a magnification of 154X was sufficient to capture images at a scale of 50 μm. The CCD camera is listed as component 6 in Figure 21.

DP 1.5 links the device to a processing system. The image taken by the CCD camera needs to be processed for profile extraction and curvature calculation. Linking the system to this external processing system allows for the design to remain portable and not require the integration of complex software. This functional requirement is represented as component 2 in Figure 21.

3.4. Prototype Production

3.4.1. Image Capture System

Due to time constraints, the extent of our device was limited to the development of a benchtop model with cost effective components. A 1 mm acrylic ball lens was affixed to an iPhone 5c camera as shown in Figure 23. Calibration tests were conducted to test the magnification and resolution of the system using a stage micrometer with 0.01 mm (10 μm) increments. Imaging an object with a known distance, such as the stage micrometer, can be used to calibrate the pixel area of the magnification system. Software called imageJ was used to determine that images taken with the magnified system contained 1980.1 pixels/mm.

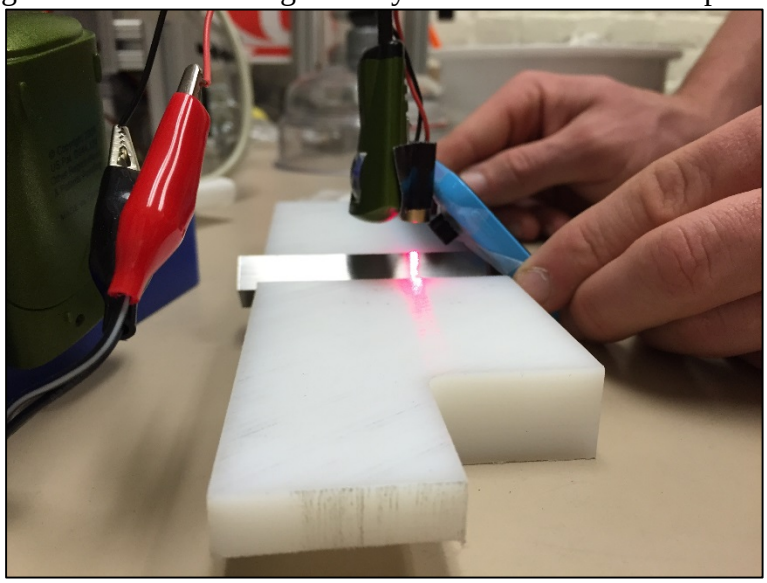

Figure 23: Benchtop optical test prototype

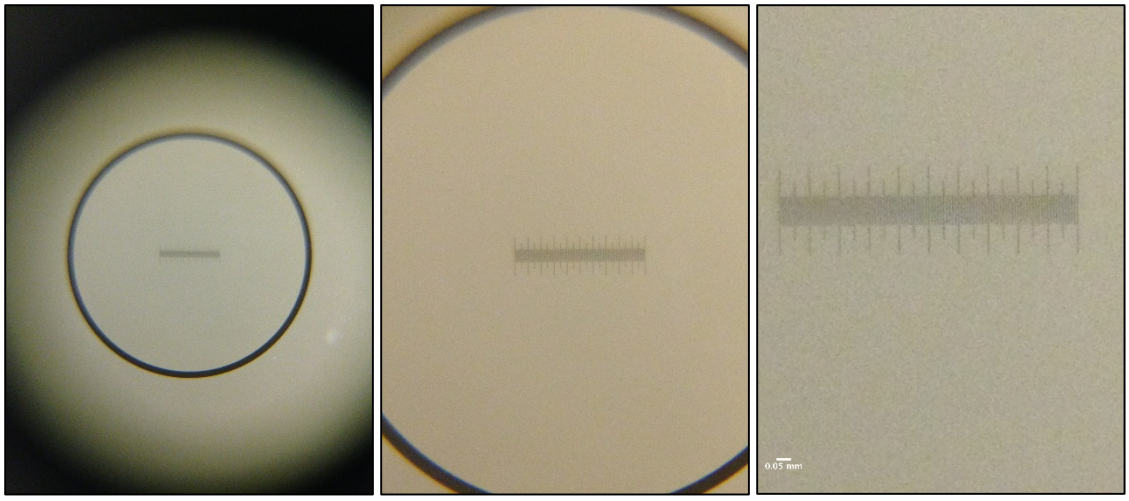

Figure 24: (L to R) Images of slide micrometer captured with iPhone 5c-lens setup with no digital zoom, 50% digital zoom, and 100% digital zoom

The 8-megapixel camera has a 33 mm focal length and a resolution of 640 x 1136 pixels and digital zoom (*Apple iPhone 5c Specs*, 2015). As seen in Figure 24 only images captured with full digital zoom, which we calculated to be 154X magnification, displayed 50-µm resolution. Magnification achieved was determined by the ratio of the pixel area of the magnified image to the pixel area of the physical camera. The calculation is expressed below (*Methods to Determine the Size of an Object in Microns*, 2015).

$$iPhone\ Specification: 326\ pixel/\ in\ =\ 0.0128\ pixel/\mu m$$
$$Pixel\ Area\ of Magnification\ System\ Images: 1980.1\ pixel\ /\ mm\ =\ 1.98\ pixel/\mu m$$
$$1.98\ pixel/\mu m\ /\ 0.0128\ pixel/\mu m\ =\ \mathbf{154}\boldsymbol{X\ magnification}$$

A 5 mW, 650 nm line laser was positioned perpendicular to the corner of the edge sample to achieve the most uniform line projection possible as seen in Figure 23. The camera was then positioned at the corner of the edge sample where the laser line was projected. Images of the line projected onto the edge such as in Figure 25 were captured.

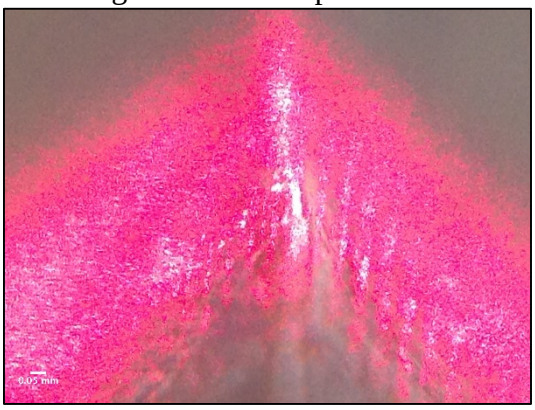

Figure 25: Laser line projected onto 8 min edge at 154X magnification

3.4.2. MATLAB Coding

A MATLAB script was created to extract the profile of an edge. The function prompts a file open window and looks for any .jpg files. Once the desired file is selected, the image can be cropped so only the desired area is used in the script. The cropped image is then ready to be run though a profile extraction function.

The script then defined the cropped image's pixel intensities and thresholded pixels corresponding to the intensity levels associated with the laser to extract the laser projection from the image. All MATLAB coding can be found in Appendix N.

3.6. Discussion

3.6.1. Accomplishments

Through benchtop testing, we determined that it might be possible to develop a system that incorporates a cell phone camera in the design. By affixing a ball lens to an iPhone camera, an image was captured at the ideal scale of 50μm. Although the captured laser stripe image was not high resolution at the selected scale, a rough edge profile was still extracted using the MATLAB script we produced.

3.6.2. Critical Assessment of Design Method

As evident from our benchtop testing, attention to the light projection specifications was overlooked. A sharper laser line is needed to capture a better image of the edge with the laser line projected onto it. Exploring higher-powered lasers, lasers with a different wavelength, or even a different light source all together, such as LEDs, could improve the line projection resolution. Overall, the profile extraction method needs further development. Emphasis on acquiring a greater resolution edge profile should be pursued.

3.6.3. Assessment of Axiomatic Design

The goal of using axiomatic design was to maximize the independence of the functional elements, followed by minimizing the information content of our device. Axiomatic design provided the opportunity to first list our design requirements and determine corresponding design parameters. This resulted in a design where the components were as robust and independent as possible. This helped ensure that all design components were independent of one another and functioned correctly. Visual models accompanying each decomposition iteration might help conceptualize iterations and expose design flaws. Overall, axiomatic design is a good way to create designs by eliminating wasteful iterations and components that overcomplicate the design.

3.6.4. Follow Up on Constraints

To satisfy our target customer, the device needs to be portable. To allow for portability, considerations need to be made for component sizing. Also, the power and computer processing systems need to be compact enough to fit within the portable design. Furthermore, a balance between component resolution and cost needs to be considered to make this affordable for our target customer.

3.6.5. Potential Commercial Uses

The design is largely applicable to ski racers and professional ski tuners for personal use. Ski and snowboard manufacturers could use this device to run quality checks on the edges of newly produced skis and snowboards, ensuring they are sharp enough for release. Ski retail shops could also use the device for a similar purpose of checking ski edge sharpness after tuning it for a customer. At a low enough retail cost the device could even be marketed to recreational skiers as a tool to identify when their skis need professional sharpening. Lastly, the design could apply to other industries such as cutting tool, sheet metal cutters, and potentially other sports that require specifically tuned edges such as luge and bobsledding.

3.7. Concluding Remarks

1. An optical system using an iPhone camera proved feasible. This suggests that a system could be designed using low cost components
2. The iPhone camera setup was able to capture an image within the ideal scale range of 50-70 μm

3. The MATLAB script was developed to extract an edge profile from the projection system image
4. The MATLAB script needs to apply associated height values with each point of the edge though optical triangulation.
5. Further work needs to be done to identify a light projection source with better resolution.

3.8. Future Work

Benchtop testing was conducted with low cost components due to time constraints. The next step is to construct a setup with optimized components within a $1000 budget. Continued work needs to be done on finding a light projection system with greater resolution then the line laser used in this testing. The edge extraction program needs additional work to utilize the triangulation principle to associate height values with the projected laser profile image so the profile can effectively be measured in CurvSoft. An integrated tracking system correlates sharpness to position along the length of the ski. For portability, an onboard power system and built-in computer-processing unit will be to also be developed. The unit should also integrate a wireless transmission system for data transfer to the post processing system. This will help realize the establishment of a user generated curvature database where users can keep track of their tuning results for different snow conditions. Finally, further consideration should be made to design the housing for manufacturability.

3.9. References

2015 SIA Snow Sports Fact Sheet. (2015, January 1). Retrieved April 26, 2015, from http://www.snowsports.org/Retailers/Research/SnowSportsFactSheet

Apple iPhone 5c specs. (2015). Retrieved April 26, 2015, from http://www.phonearena.com/phones/Apple-iPhone-5c_id7983

Chen, X., Zhang, G., & Sun, J. (2013). An Efficient and Accurate Method for Real-Time Processing of Light Stripe Images. *Advances in Mechanical Engineering, 5*. doi: 10.1155/2013/456927

Crampton, S. J., & Champ, P. (2009). Optical Scanning Probe: Google Patents.

Gleason, K., Lemoine and Brown. (2013). Profile Curvatures by Heron's Formula as a Function of Scale and Position on an Edge Rounded by Mass Finishing.

Henrikson, P. (2009). Method and a device for measurement of edges: Google Patents.

Kumar, S., Tiwari, P. K., & Chaudhury, S. B. (2006, 15-17 Dec. 2006). *An optical triangulation method for non-contact profile measurement.* Paper presented at the Industrial Technology, 2006. ICIT 2006. IEEE International Conference on.

Methods to determine the size of an object in microns. (2015). Retrieved April 26, 2015, from http://openwetware.org/wiki/Methods_to_determine_the_size_of_an_object_in_microns

Sieckmann, F. (2015). Microscope with wireless radio interface and microscope system: Google Patents.

Smith, Z. J., Chu, K., Espenson, A. R., Rahimzadeh, M., Gryshuk, A., Molinaro, M., . . . Wachsmann-Hogiu, S. (2011). Cell-Phone-Based Platform for Biomedical Device Development and Education Applications. *PLoS ONE, 6*(3), e17150. doi: 10.1371/journal.pone.0017150

Svetkoff, D. J., Rohrer, D. K., & Kelley, R. W. (1997). Triangulation-based 3D imaging and processing method and system: Google Patents.

Appendix A: Microscope Procedure

- Open the LEXT software on the lab computer desktop
- Turn on the microscope and change setting to the laser option
- Place an edge sample in the orienting block onto the microscope tray within the cameras field of view and make sure the edge is vertical in orientation
- Focus with the x10 lens using the hand adjustment on the side of the microscope and lock the focal position
- Next, cycle through all the lens, focuses at each one along the way, until arriving at the 50x magnification level
- Identify the depth range that the measurement and set the top and bottom focal lengths in the LEXT software
    - Try to get a generous amount of the edge in the measurement frame, The makes leaves more room to measure with larger scales later
- Decrease the light level in the image when the microscope is focused on the tip of the edge to reduce the presence of red indicators which mark places where the image will become distorted because of too much light
- Close the door to the microscope room and shut off the lights to run the rendering process
- Save data with information rich names (type of sample, magnification level, what is seen in image “nick”, etc.)
- Copy the saved data to the Research Drive.

Appendix B: Testing Setup

- Make sure the screw valves are closed and attach the air supply hose to the adapter located on the valves’ plate.
- Load the desired edge sample into polyethylene holding bar and tighten bolt and nut that holds it in place.
- Set the angles of the edge holders by inserting a pin through the holes on the holders and through a hole on the pegboard behind it. Angles 30, 45, and 60 degrees can be set using the peg boards, 15 degrees needs to be measured using a protractor and tightened down against the frame with the nut on the axis of the holder.
- Insert the holding bar into the edge holding claws and hand-tighten the screws of the holder pads.
- Load a surfaced testing material into the material cavity in the tester and turn the tangential pneumatic cylinder to tighten the head of the cylinder to the material block and hold it in place.
- Turn the tangential cylinder valve slowly to allow some air pressure to build and move the testing block forward on its supporting rails until it reaches the first indicator line.
- Slowly turn the normal cylinder valve to move the testing block down until the testing material barely comes in contact with the edge sample.
- Adjust the balance of the edge sample holder to make the edge surface flat against the testing material and tighten the holder screws with an allen wrench.

Appendix C: Testing Procedure

- Now that the edge sample is properly balanced at the desired edge angle, load a block testing material with the proper geometry into the material cavity (try to use the same

block of testing material each time if it can be easily refinished to maintain the balance set on the edge)

- Apply pressure to the tangential cylinder until the testing block moves up to the first indicated line on the rail.
    - If the testing block moves past the first indication line, release the pressure in the cylinder to bring it back to the resting position and start again
- Apply pressure to the normal cylinder to bring the testing block down until the testing material comes in contact with the edge sample. (check to make sure the whole edge surface is in contact with the material) Then continue to add pressure to the normal cylinder until the pressure gauge reads the desired pressure.
- Start turning the tangential value slowly to apply more pressure in the tangential direction and watch both the testing block and the pressure gauge as you do so.
- Record the pressure reading on the gauge when the tester block reaches the second reference line on the rail when the edge sample defeats the material
    - When the edge defeats the material it will either jump to the second line or slowly move across the material
    - When the tester jumps the pressure gauge will jump to another pressure because of the rapid expansion of the cylinder. The proper value to record is the pressure seen on the gauge before the jump, this is why you need to be watching the gauge and the testing block at the same time.
    - When the material moves slowly you might need to continue to apply enough pressure to make it all the way to the second reference line.

Appendix D: Tester Maintenance

To keep the tester operating effectively maintenance was performed after successive testing. The groove of the rails that the testing block runs on should be cleaned and lightly oiled. This is to make sure that the testing block is able to slide freely across the rails and so that the testing data is not seriously affected by the friction in the testing block's movements. Use a small cotton swab and apply a small amount of silicon based oil to the tip and run the wetted swab up and down the grooves in the rails until they are clean and the rail is lubricated. Do not over lubricate, lubrication in a friction testing environment can ruin test data.

Constantly check the hose connections for leaks. The connections are snap links that are tightened with Teflon tape but the connections are not always perfect. The snap links allow the hose connection to rotate to prevent entanglement in the lines but they forgo creating a proper seal. For the most part the hose connections work well, especially under pressure, but often they spring slow leaks that you can't hear but you can see because the pressure gauge slowly falls after setting the pressure to a certain level. No testing should be performed with the presence of an air leak.

The large nut around the tangential cylinder that holds the cylinder to the frame should remain loose but tight enough not to have too much play during testing. This connection needs to remain loose so the cylinder can travel up and down as the testing block does to maintain a straight application of force.

Appendix E: Solid Models Used for Machining

Corresponding files located at: \\research.wpi.edu\Surflab\2014-2015\Projects\Edge MQP\Appendix E

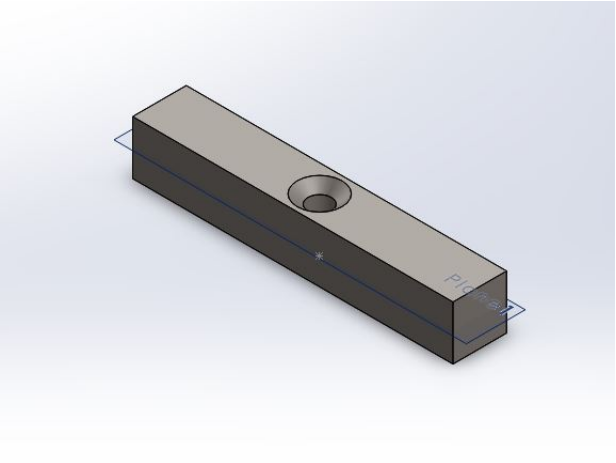

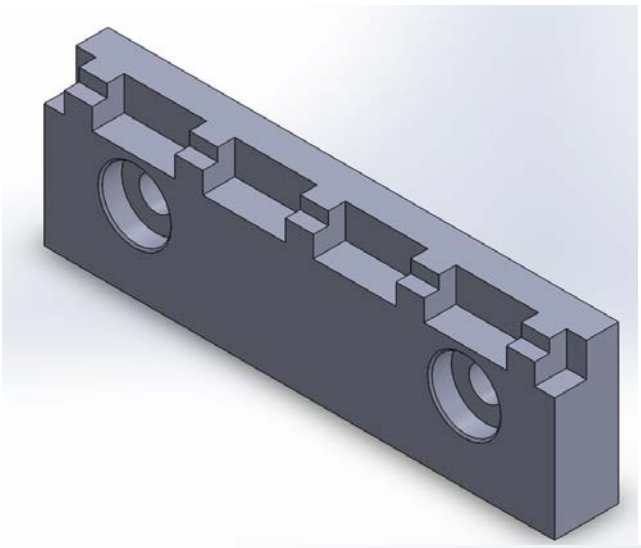

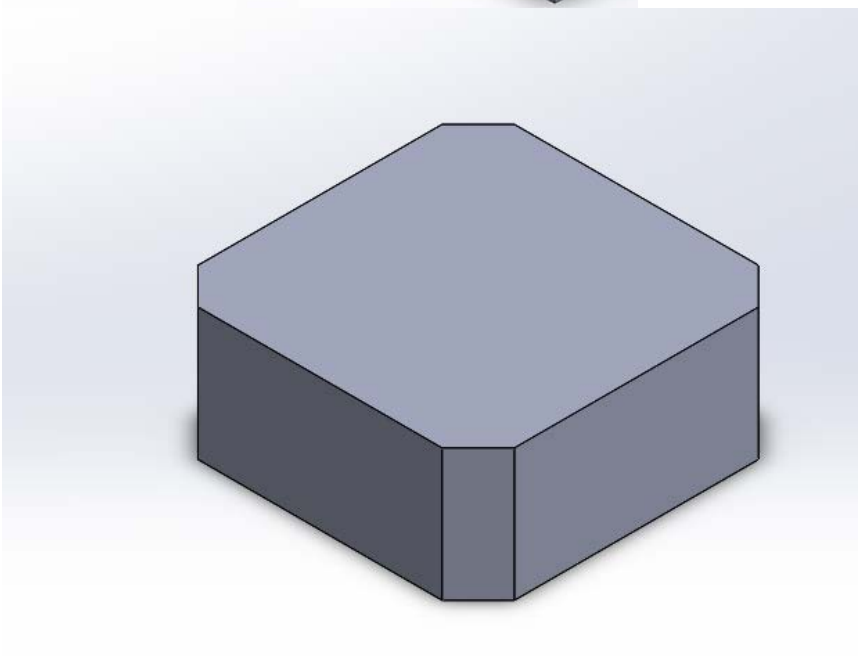

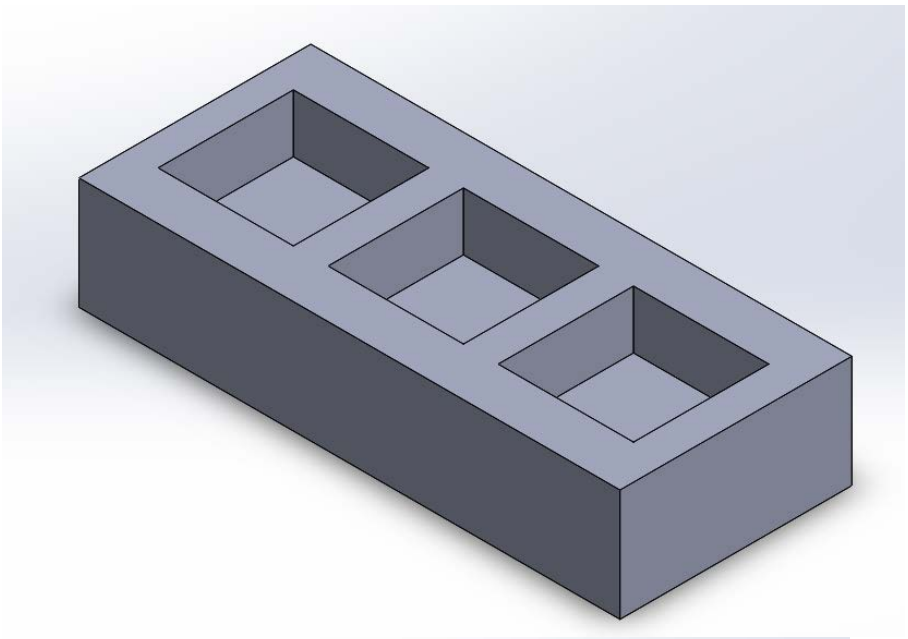

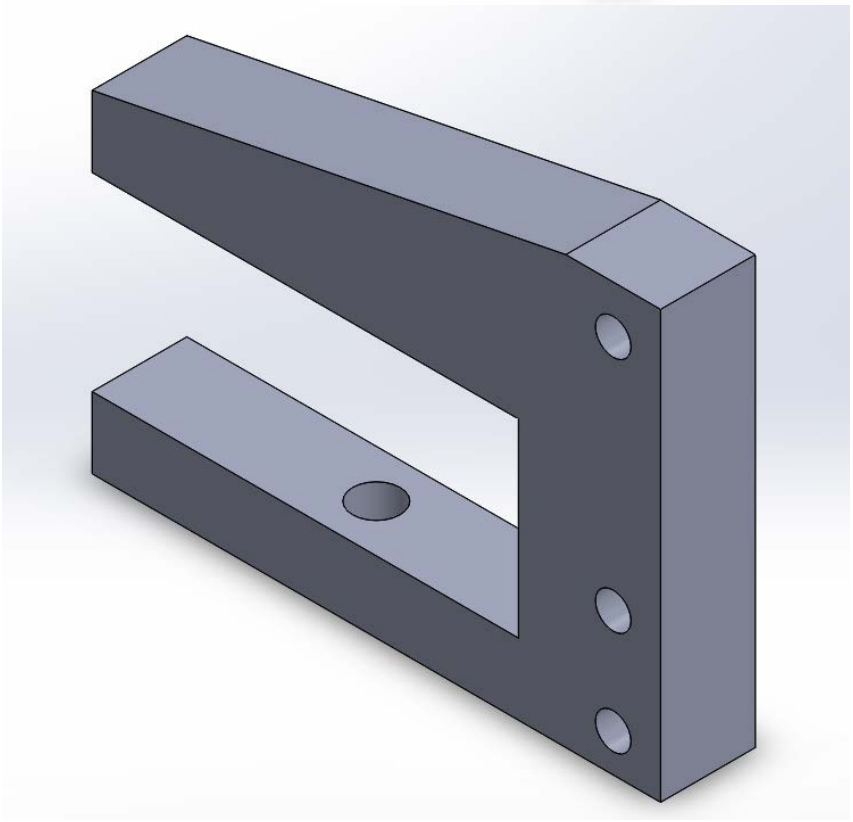

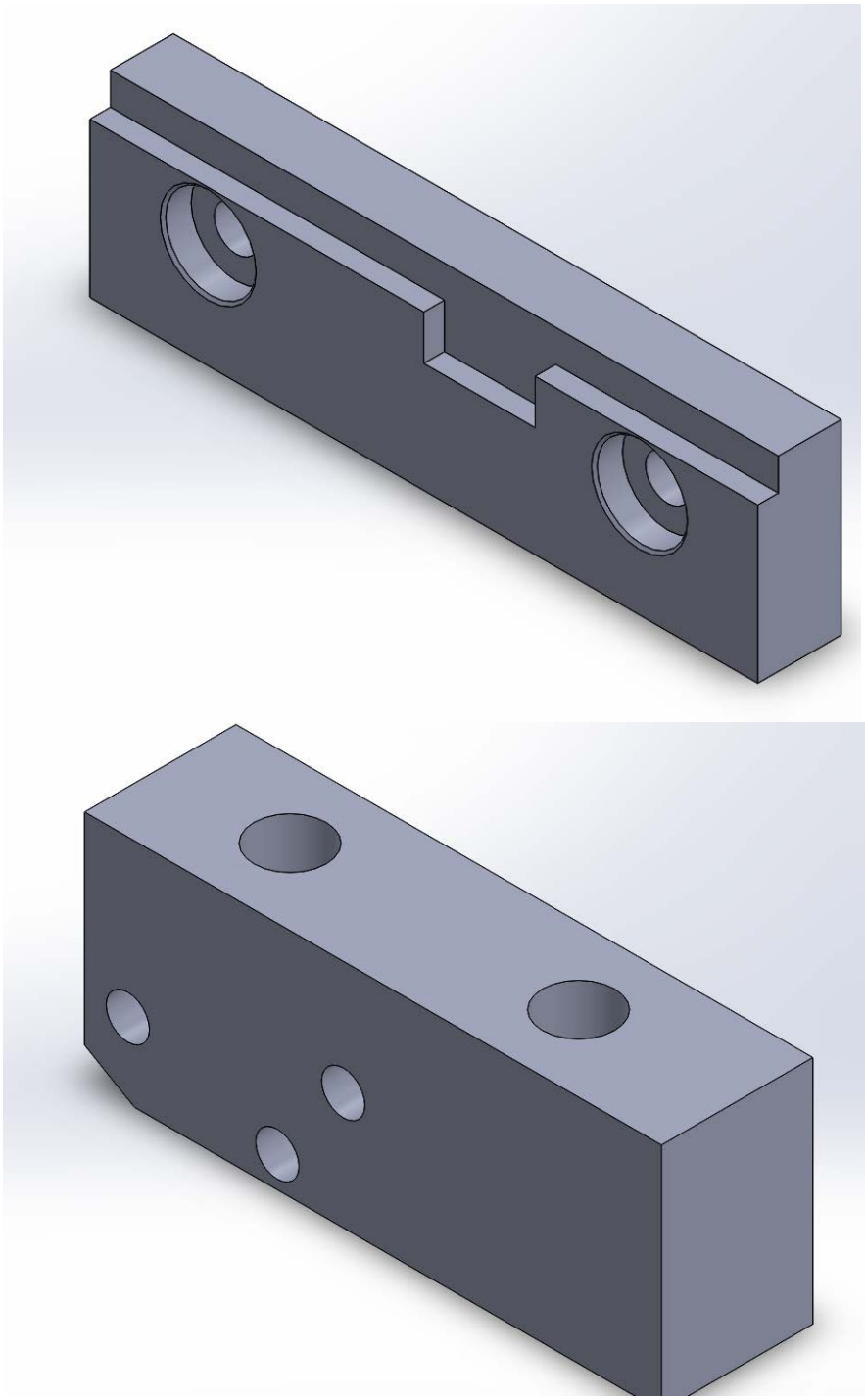

Appendix F: Machining

Corresponding files located at: \\research.wpi.edu\Surflab\2014-2015\Projects\Edge MQP\Appendix F

We first created a solid model of the prisms for use in Esprit to program the CNC machine. Tooling was selected to create the simulated ski edges: 3/8” Ferrous End Mill, 3/8” Center Mill, #10 Drill, and an 82 degree countersink. These were selected based on the current setup of the ski edge tester. Next, CAM programs were created in Esprit to face all of the sides of the edge sample, drill the hole, and countersink each side. To help reduce cycle time on the

milling of the sides of the edge, a fixture was developed to provide clearance on all sides of the edge sample so that three sides of the edge could be milled in one operation.

From the block of stock, prisms the approximate size of 2.75” by 0.5” by 0.5” were cut on a horizontal bandsaw. Next, one of the rectangular faces and both ends were faced on the mill. Using the edge holding fixture we created, the other three rectangular faces were milled. A drilled hole, followed by a countersink, were added to two opposing rectangular faces of the prism. This would be used to secure the prism to the testing apparatus allowing the simulated ski edge on the prism could be used repeatedly without fail. After the edges were milled, all the edges were finished using a SKS rubber edge deburrer to remove the burr created by machining.

Machining Programs:

Edge Stage 1:

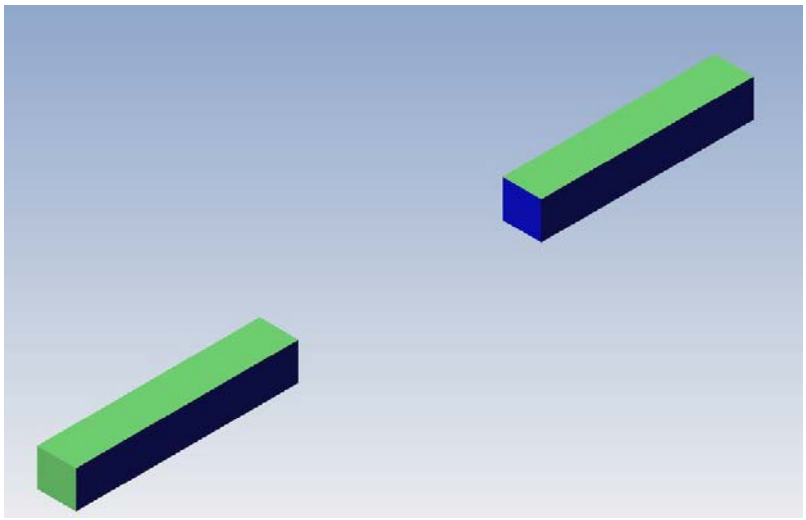

Edge Stage 2:

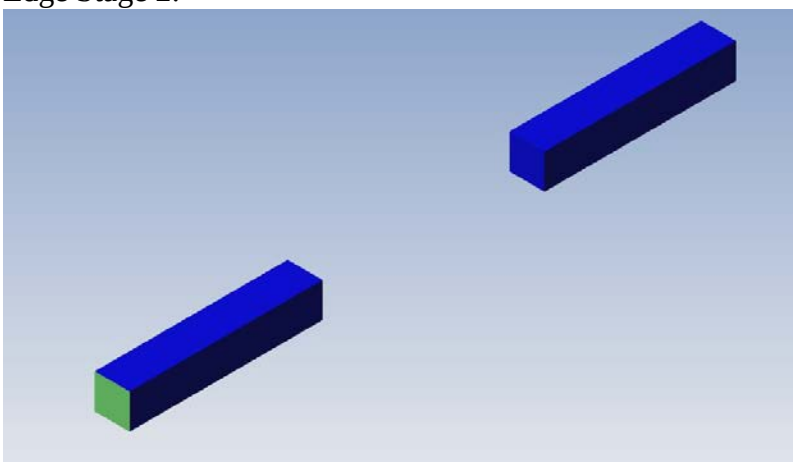

Edge Stage 3:

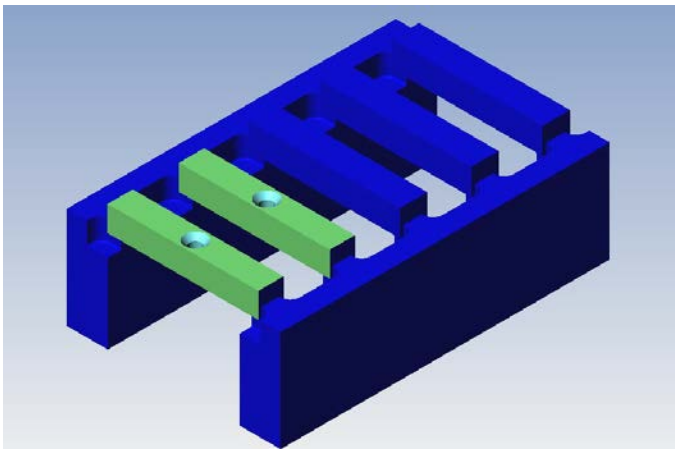

Edge Stage 4:

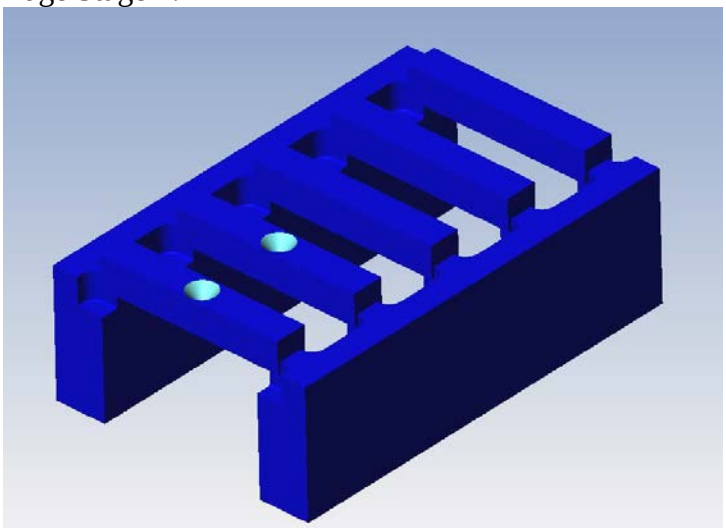

Edge Soft Jaws:

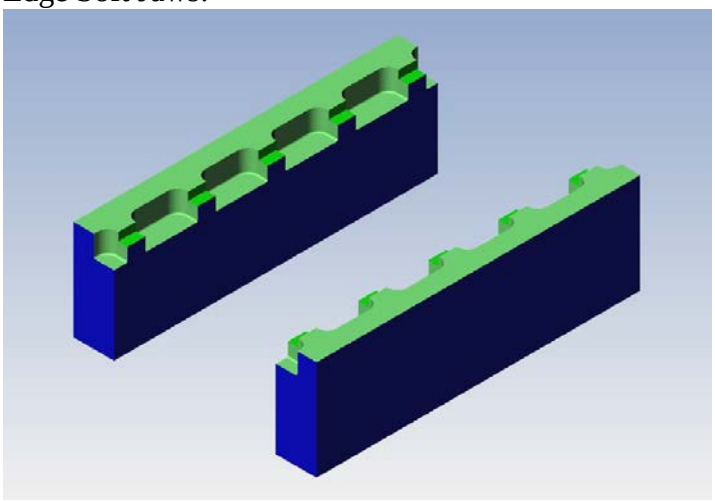

Pinboard Part 1:

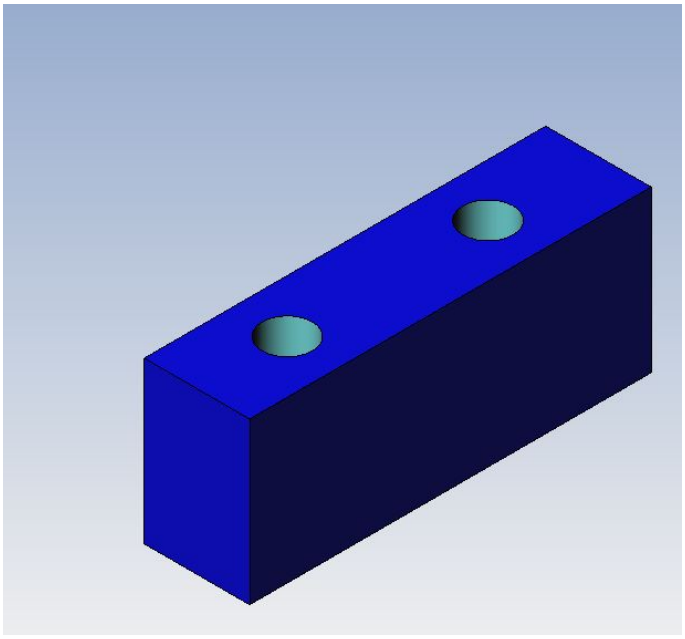

Pinboard Part 2:

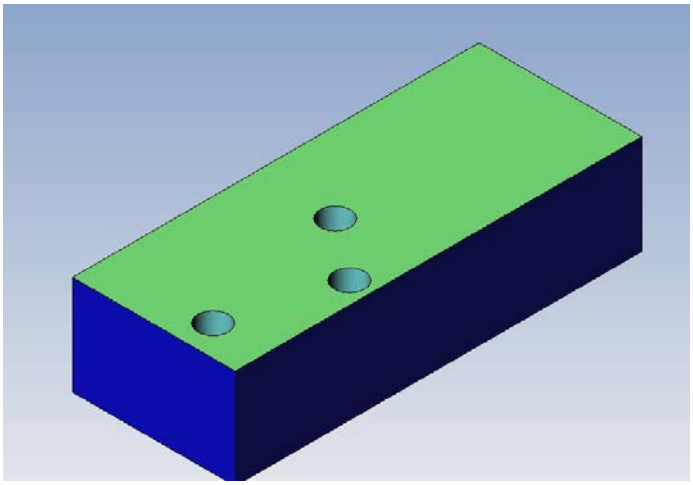

Pinboard Part 3:

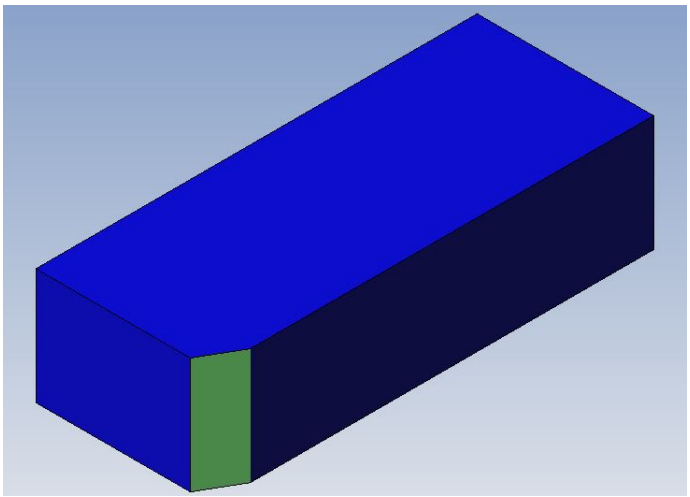

Pinboard Soft Jaw:

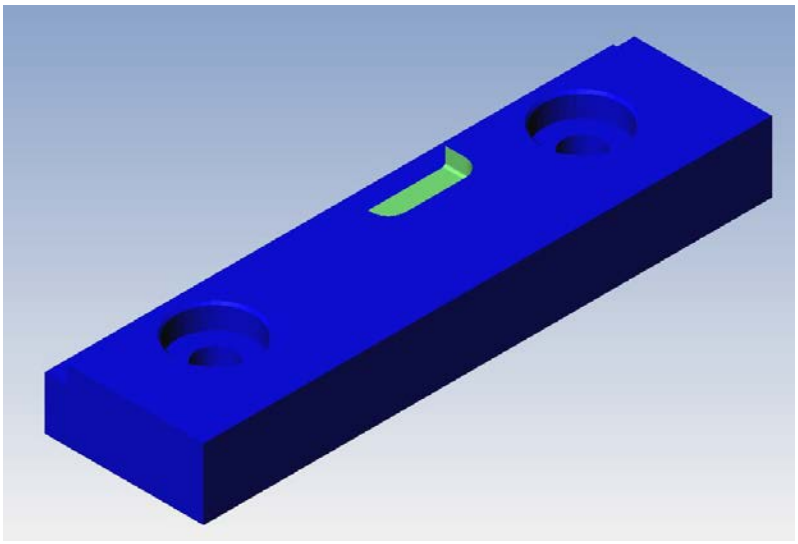

Clamp Holes:

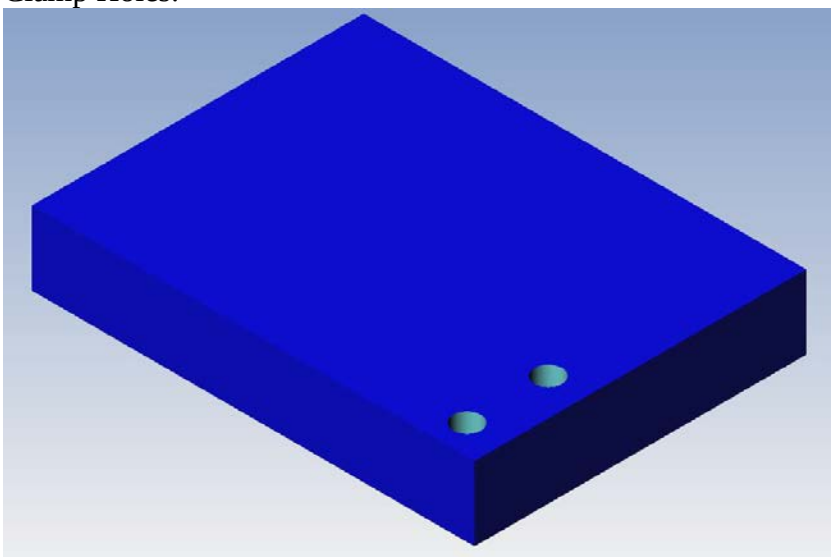

Tester Frame Holes:

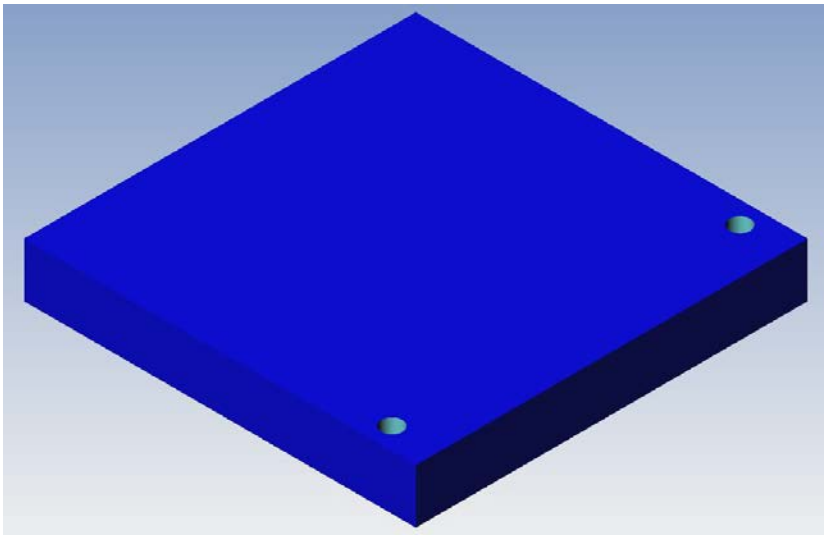

Machinable Wax Stage 1:

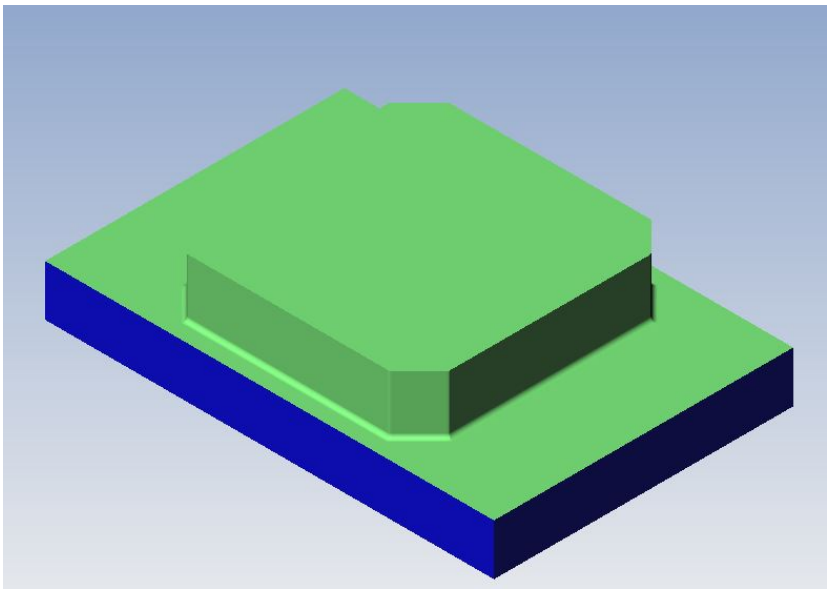

Machinable Wax Stage 2:

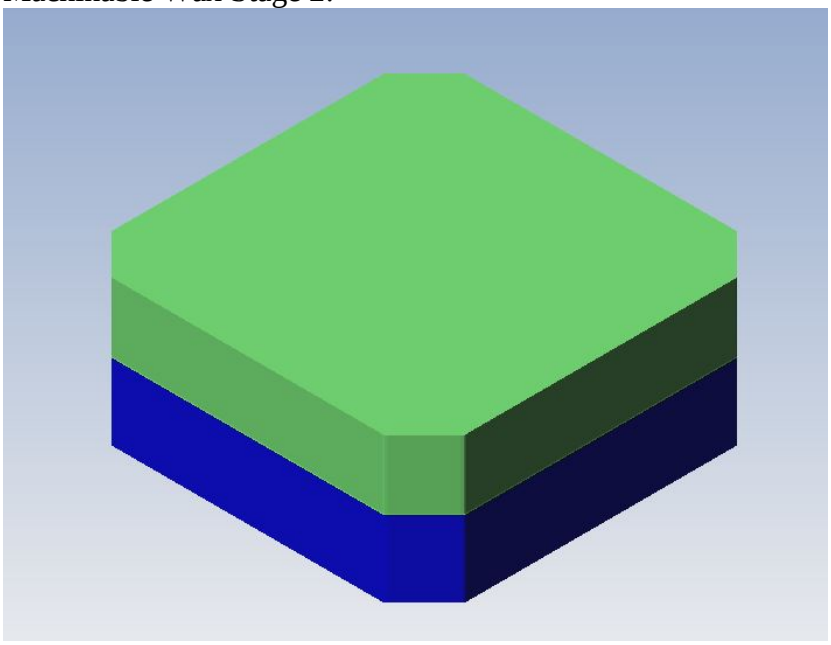

Machinable Wax Facing Operation:

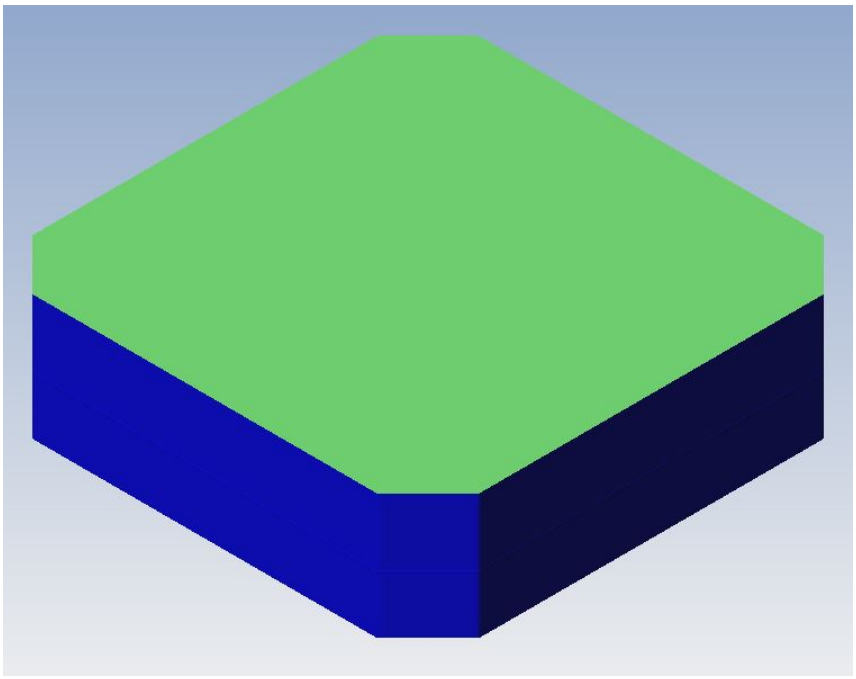

Appendix G: Other Performance Graphs

Corresponding files located at: \\research.wpi.edu\Surflab\2014-2015\Projects\Edge MQP\Appendix G

Polyethylene:

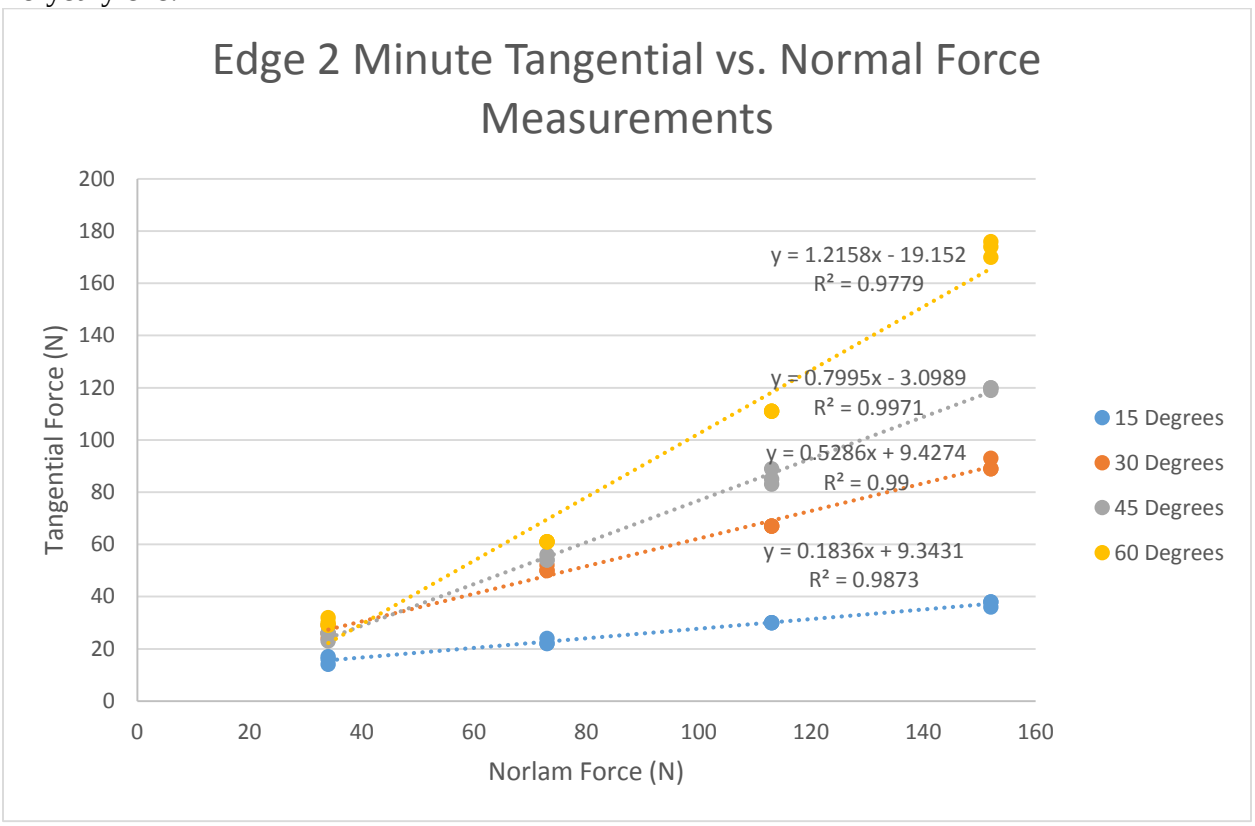

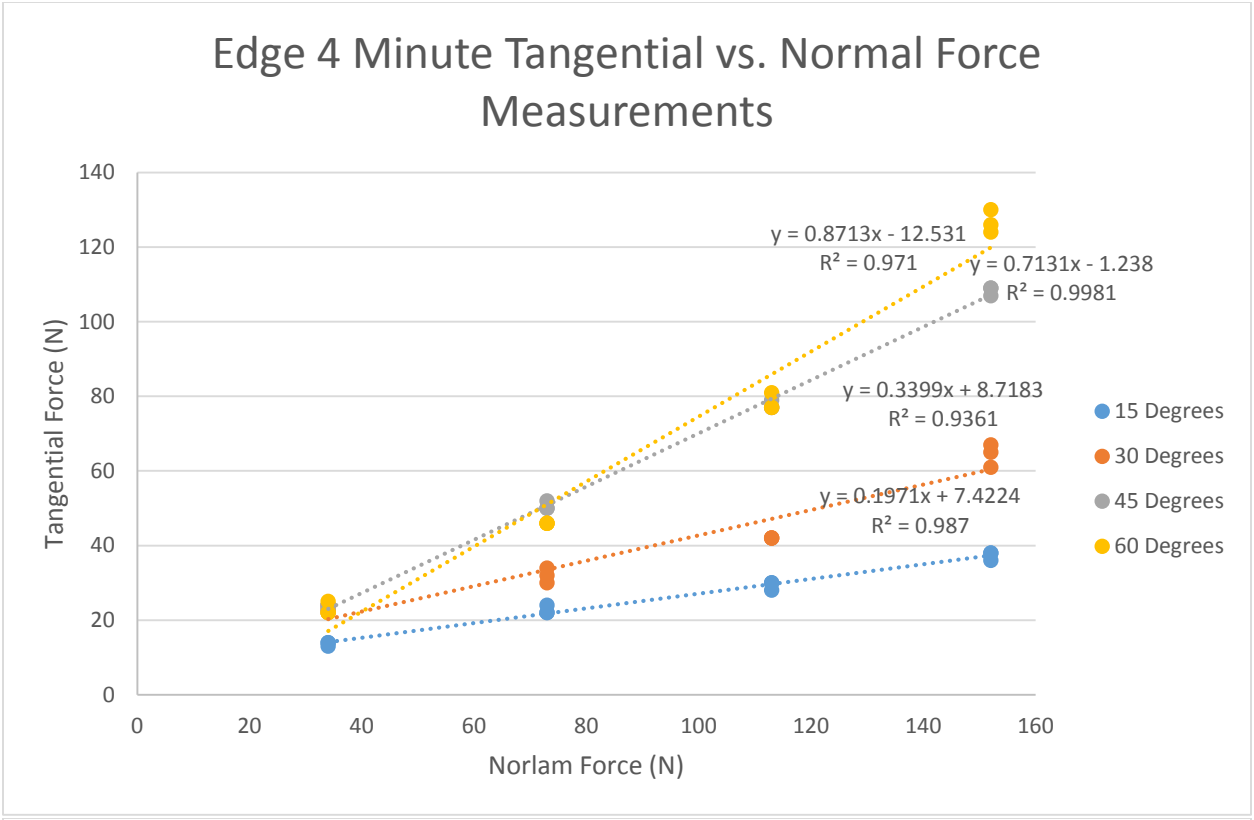
Edge 4 Minute Tangential vs. Normal Force Measurements
Tangential Force (N)
Norlam Force (N)
y = 0.8713x - 12.531
R² = 0.971
y = 0.7131x - 1.238
R² = 0.9981
y = 0.3399x + 8.7183
R² = 0.9361
y = 0.1971x + 7.4224
R² = 0.987
15 Degrees
30 Degrees
45 Degrees
60 Degrees

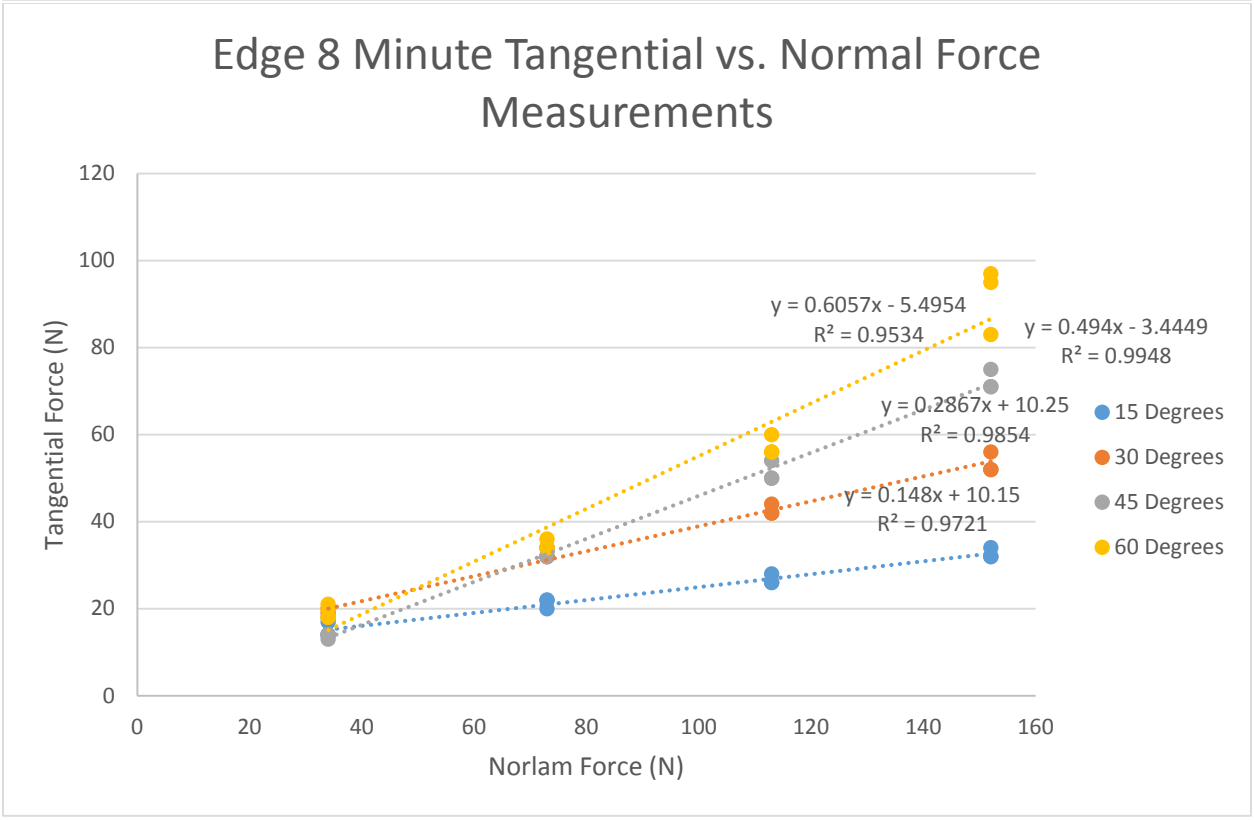
Edge 8 Minute Tangential vs. Normal Force Measurements
Tangential Force (N)
Norlam Force (N)
y = 0.6057x - 5.4954
R² = 0.9534
y = 0.494x - 3.4449
R² = 0.9948
y = 0.2867x + 10.25
R² = 0.9854
y = 0.148x + 10.15
R² = 0.9721
15 Degrees
30 Degrees
45 Degrees
60 Degrees

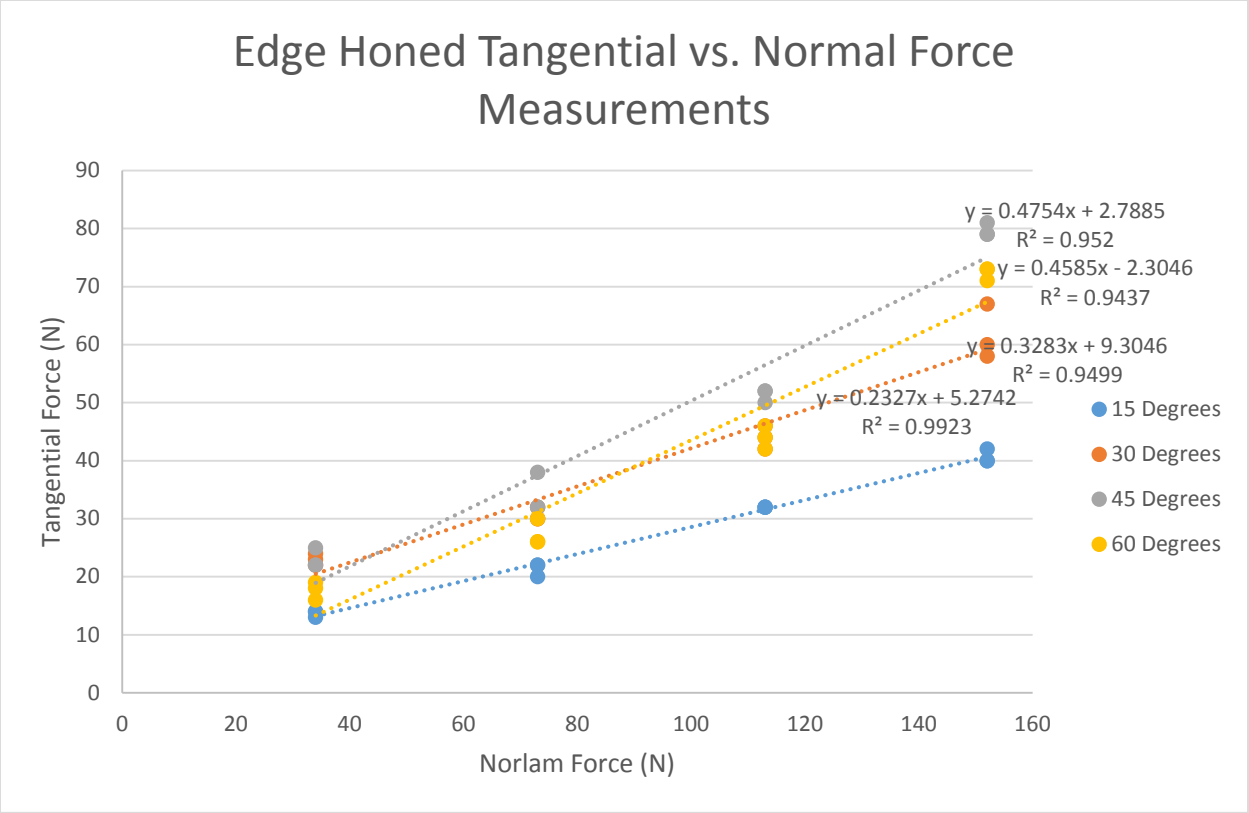

Machinable Wax:

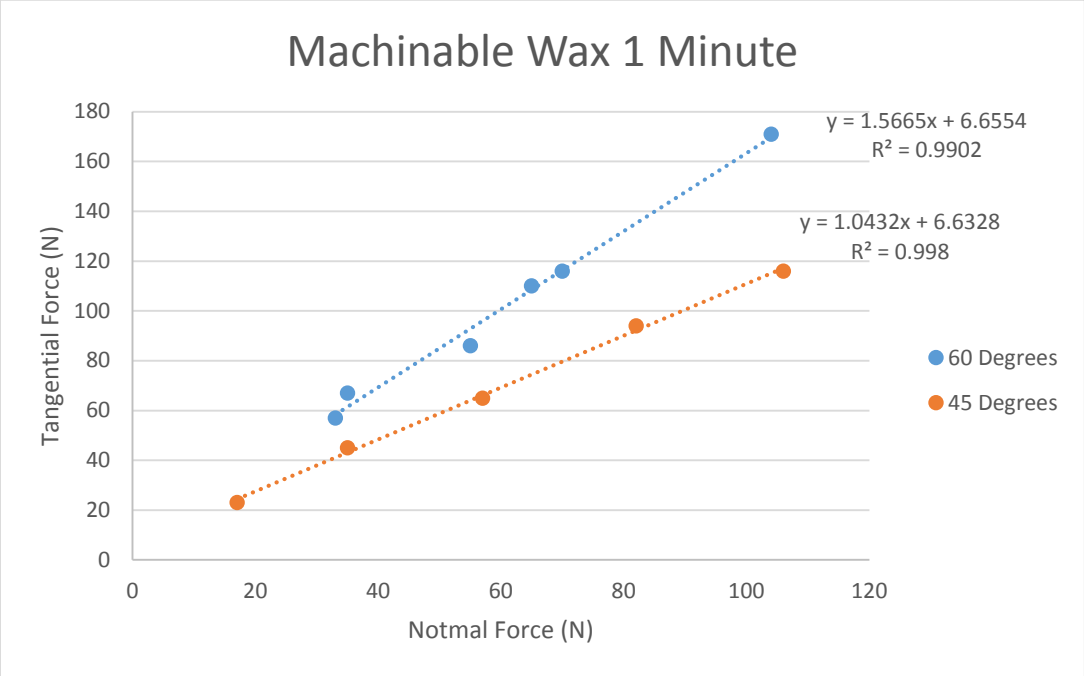

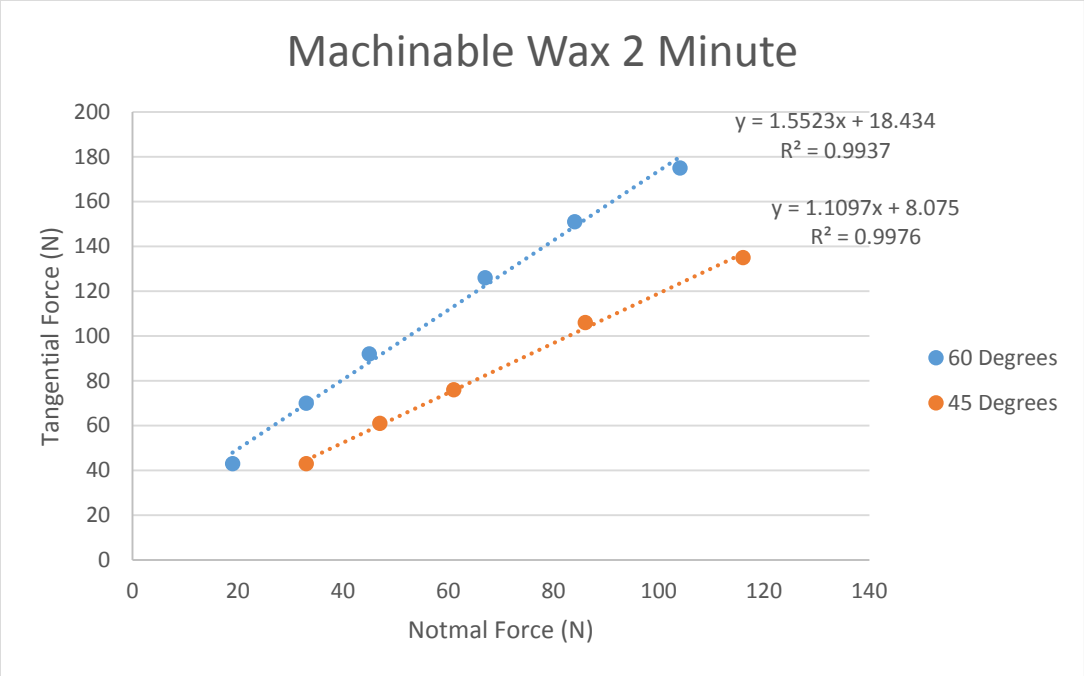
Machinable Wax 2 Minute
y = 1.5523x + 18.434
R² = 0.9937
y = 1.1097x + 8.075
R² = 0.9976
Tangential Force (N)
Notmal Force (N)
60 Degrees
45 Degrees
0
20
40
60
80
100
120
140
160
180
200

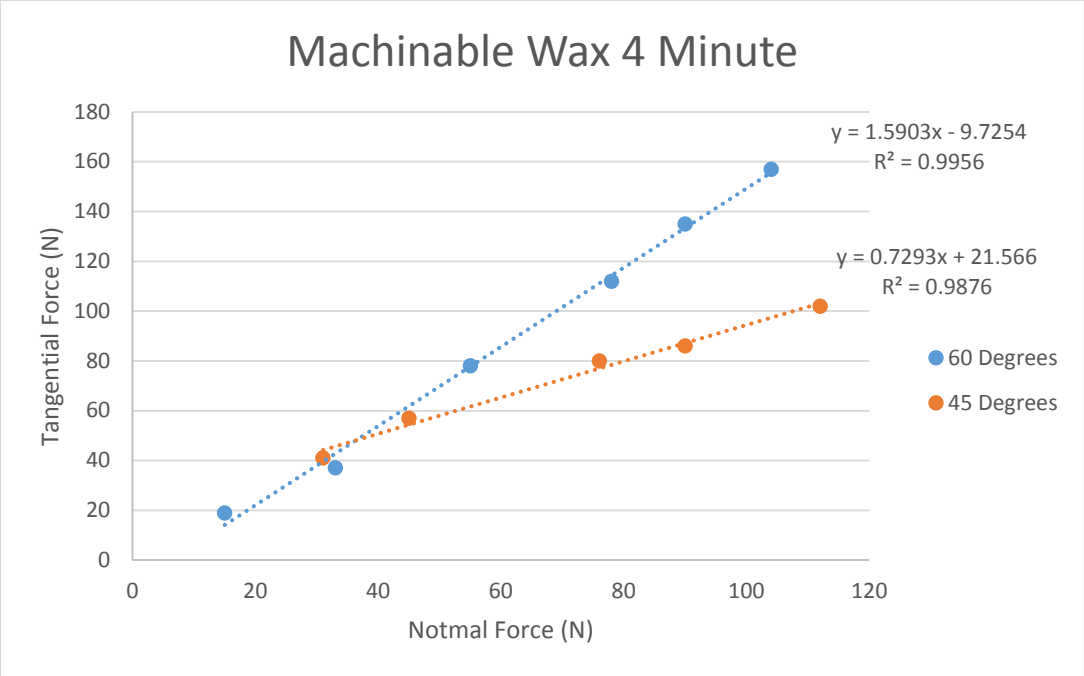
Machinable Wax 4 Minute
y = 1.5903x - 9.7254
R² = 0.9956
y = 0.7293x + 21.566
R² = 0.9876
Tangential Force (N)
Notmal Force (N)
60 Degrees
45 Degrees
0
20
40
60
80
100
120
140
160
180

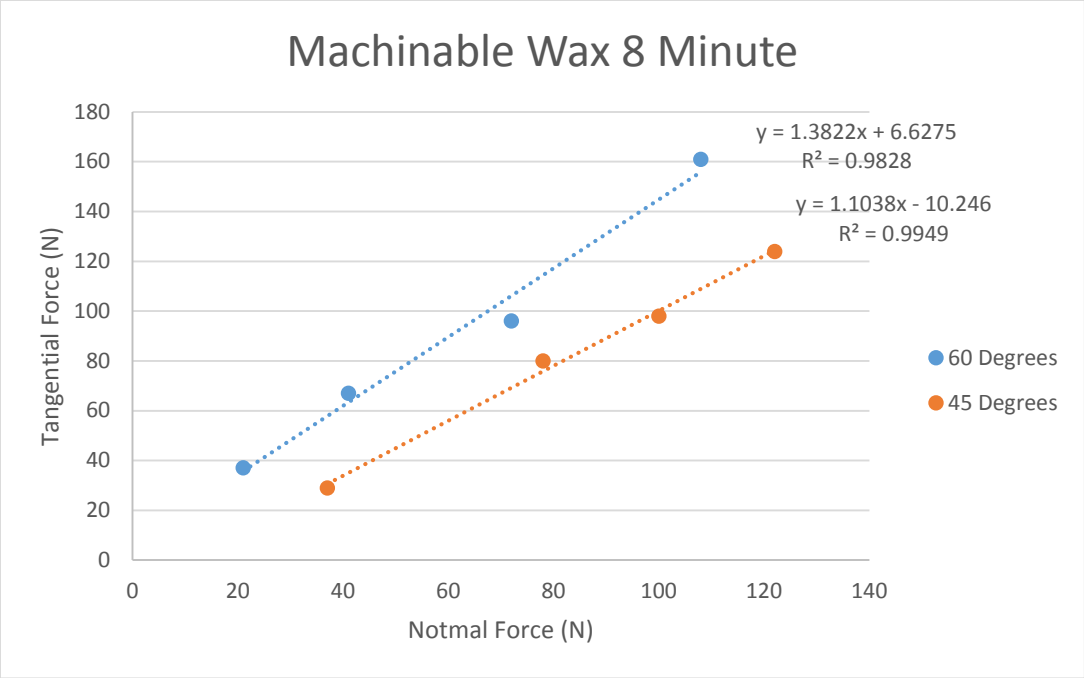

Appendix H: Curvature Graphs

Corresponding files located at: \\research.wpi.edu\Surflab\2014-2015\Projects\Edge MQP\Appendix H

Appendix I: Curvature Analysis

Corresponding files located at: \\research.wpi.edu\Surflab\2014-2015\Projects\Edge MQP\Appendix I

Next, we investigated if there is a correlation between the performance and curvature data. We broke the performance data down by the angle that the tests were taken: 15, 30, 45, and 60 degrees. From here, we then created graphs comparing the performance data versus the absolute minimum curvature at one specific scale, starting at 10 µm and moving up in increments of 5 µm until 90 µm. For each of these graphs we extracted four data points; x-coefficient from each of the 1, 2, 4, and 8 minute mass finished edges', tangential versus normal force graphs at each specific angle, and the absolute minimum curvature for each of those edges. For example, we paired the x-coefficient value from performance testing for the 2-minute mass finished edge and this was paired up with the absolute minimum curvature value for the same edge sample at a specific scale.

As the scales changed, so did the curvature values; however, the performance data stayed the same throughout all the different scales for the particular angle of testing. For each force versus curvature graph of points, we calculated the R^2 value for an exponential trend line. We recorded the R^2 value at each scale in a table. Once we went through all the scales, we created a scatter plot of the R^2 versus scale for each grouping of graphs based on angle. For example, one graph was just all the R^2 values taken from the 15 degree force tests. From here, we were able to see at which scale had the highest R^2 values. Generally, the graphs were almost parabolic shaped with a hump somewhere in the middle of the scales. With these graphs, we were able to determine at which scale we got the best correlation between the measured forces from the tester and the calculated curvature of the edge used during that specific force tests.

Once there is there is a 3D measurement of the ski edge, data can further be extracted using Mountains, Outliers, and CurvSoft computer software. Previous students working in WPI's Surface Metrology Lab developed the second two programs.

The microscope measurement files are first brought into Mountains where the measurements are shown in 3D. The first step is to separate the layers of information captured in the .lext file. There is a topography, color, and intensity layer, however we only need the topography layer. This can be extracted via the Operators tab. Next, the file needs to be cropped to only contain parts of the edge measurements. The edges did not take up the entire scanning window and therefore there are fuzzy areas around the actual edge in the measurements were the microscope tried picking up an edge where there was none. These must be cropped out so the real edge can be the only thing being picked up. This cropped measurement must be saved as a .sur, surface format.

The next step is eliminating Outlier points from the measurements. No matter how good the measurement resolution, there will still be random spiked points of data and these must be smoothed out so that further data manipulation is not skewed. To remove these, we import the surface files into the Outlier Program. Within this program, we can choose how aggressive we want the Outlier filter to be depending on the state of the surface. This filter removes the peaks from the 3D surface measurement, leaving gaps. This file is then saved as a surface in the Outlier Alpha format (check on this).

The next step is opening the Outlier-filtered surface back in Mountains. From here we can use a Modifier (check this) in order to further remove points that are in the upper 0.5% of measured points and set them as the lowest points. These areas now become non-measured points. This step further helps to eliminate outlier points that might have been missed in the previous step. From here we can use another Modifier that fills in all the non-measured points on the surface measurement to be the average of the surrounding measured points. This creates a smooth profile once again. From here, a 2D profile can be extracted from the 3D surface. Extracting Profile feature can be used, but it's important to keep a few things in mind during this step. 1) Pay attention to the orientation of the measurement. When we used the microscope we tried to keep the samples as vertical as possible, but even still some of the samples came out slightly skewed. When taking the profile, align the extracting line so that it's perpendicular to the edge, not perpendicular to the measurement. 2) Pay attention to the start and stop points on the extracted profile because sometimes it's reverse of the actual orientation of the edge. This can be changed with a simple button toggle. 3) You can slide the profile across the whole sample of the edge. Do this to find one that has a clear profile. From the previous steps, we tried to remove all the outlier points, but there still might be a few rough spots. Once a clear profile has been extracted, save this as a .txt file format.

In this final step, we use a software to calculate curvature called CurvSoft. It needs to be downloaded to the desktop in order to work because using it from the hard drive directory doesn't always work. Additionally, it can only run on computers that have Java. Upon opening the program it will ask to choose a unit – select micrometers – the software will only ask for this once, so choose correctly. From the File menu, open the .txt file as a profile. Select the Calculus Heron Hybrid Curvature for the method for calculating curvature because it will be the most accurate. For scale, write "all". We chose this for our research because we were not sure at what scale we'd find the optimal curvature so we wanted to investigate as many as we could. Curvature is calculated across the 2D profile starting at a scale of .5 micrometers up to approximately 100 micrometers in increments of .5 micrometers. The upper limit of scale was

dependent on the original depth of the topographical measurement taken. The shallower topographical depths resulted in lower scale simply because the horizontal length of the measurement was smaller. The program outputs the scale and correlating curvature measurements as 2D coordinates in a .csv file format.

The .csv files were then imported into Excel. Starting at a scale of 10 micrometers and moving up in increments of 5 micrometers, we found the minimum curvature at each of these scales. The smallest curvature relates to the largest radius, so by taking the smallest curvature, we know that all other points along the edge will only be sharper. Most of these curvature values were negative as a result of how we took the measurement, therefore these values were then taken as absolute values in order to make correlations in the future steps easier to understand.

Appendix J: T/N vs. Angle Graphs

Corresponding files located at: \\research.wpi.edu\Surflab\2014-2015\Projects\Edge MQP\Appendix J

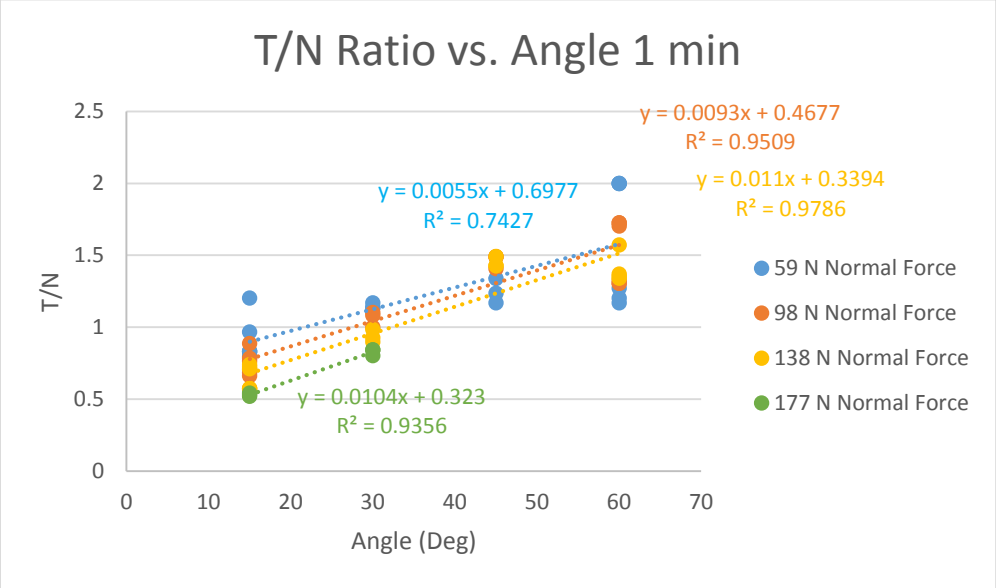

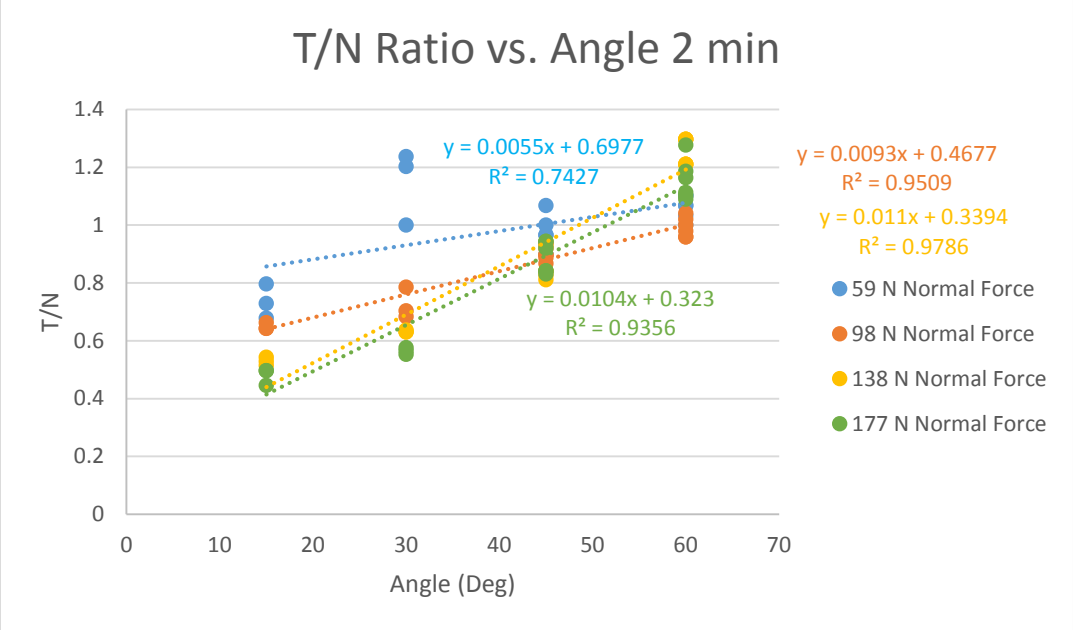

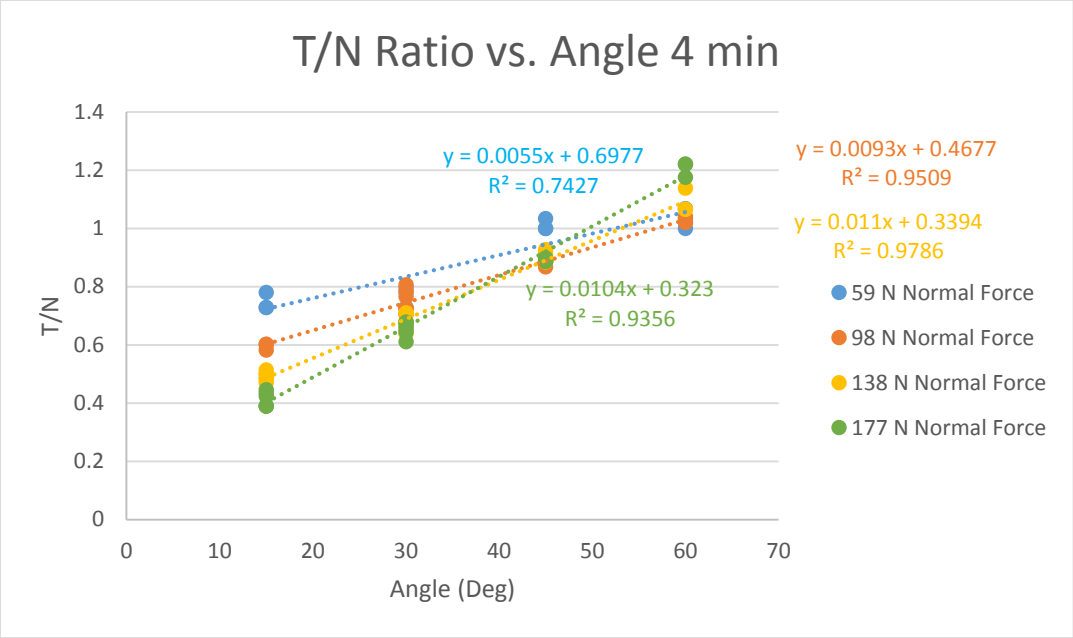
T/N Ratio vs. Angle 4 min
y = 0.0055x + 0.6977
R² = 0.7427
y = 0.0093x + 0.4677
R² = 0.9509
y = 0.011x + 0.3394
R² = 0.9786
y = 0.0104x + 0.323
R² = 0.9356
59 N Normal Force
98 N Normal Force
138 N Normal Force
177 N Normal Force
T/N
Angle (Deg)
0
0.2
0.4
0.6
0.8
1
1.2
1.4
0
10
20
30
40
50
60
70

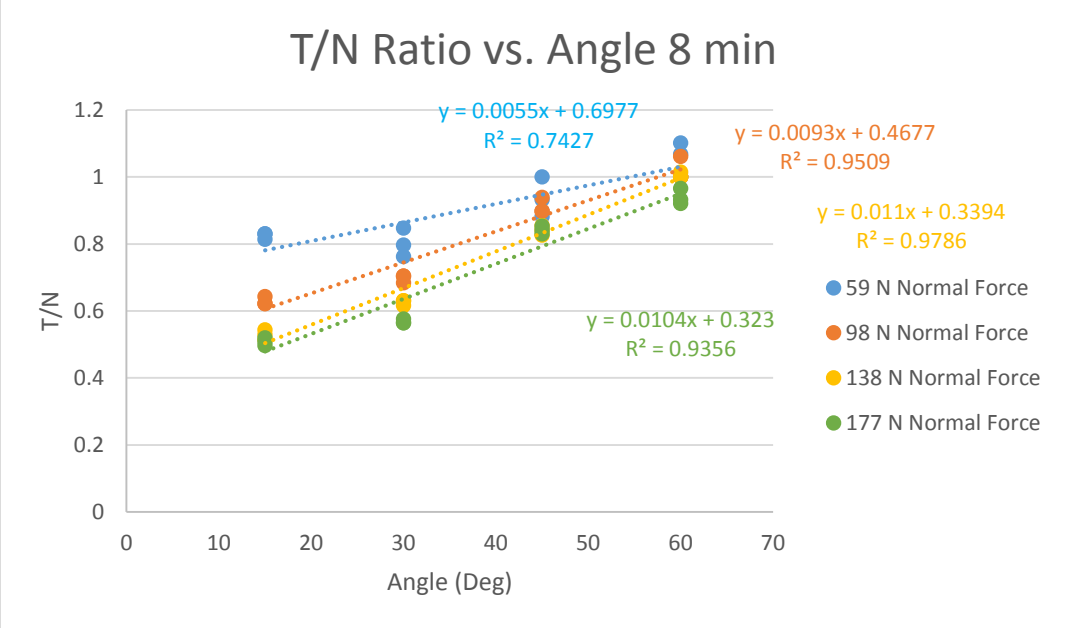
T/N Ratio vs. Angle 8 min
y = 0.0055x + 0.6977
R² = 0.7427
y = 0.0093x + 0.4677
R² = 0.9509
y = 0.011x + 0.3394
R² = 0.9786
y = 0.0104x + 0.323
R² = 0.9356
59 N Normal Force
98 N Normal Force
138 N Normal Force
177 N Normal Force
T/N
Angle (Deg)
0
0.2
0.4
0.6
0.8
1
1.2
0
10
20
30
40
50
60
70

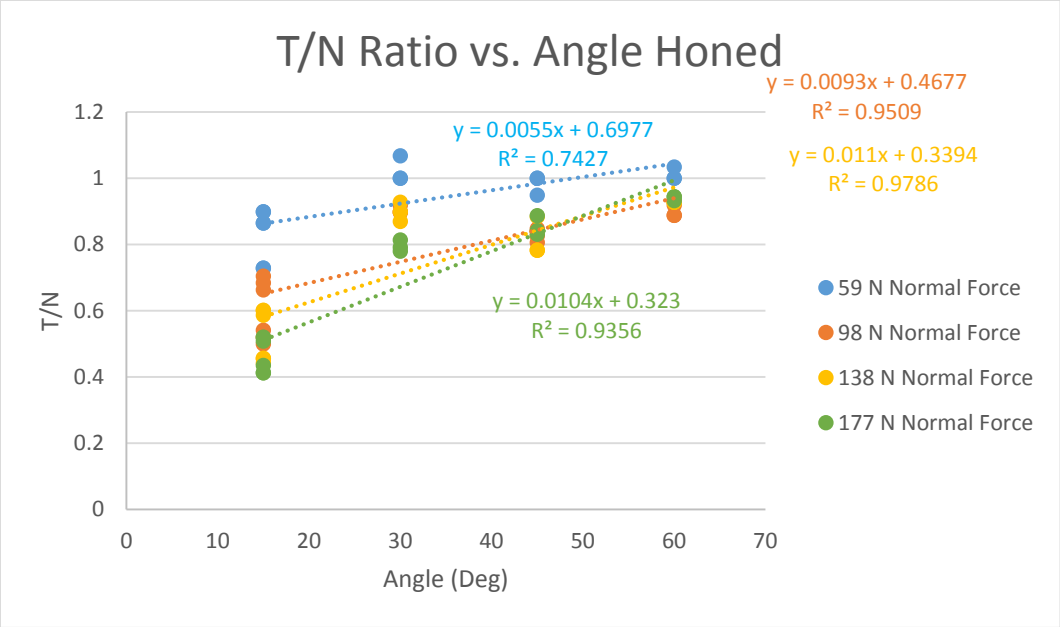

Appendix K: Data Taken with Burr Present on Edges

Corresponding files located at: \\research.wpi.edu\Surflab\2014-2015\Projects\Edge MQP\Appendix K

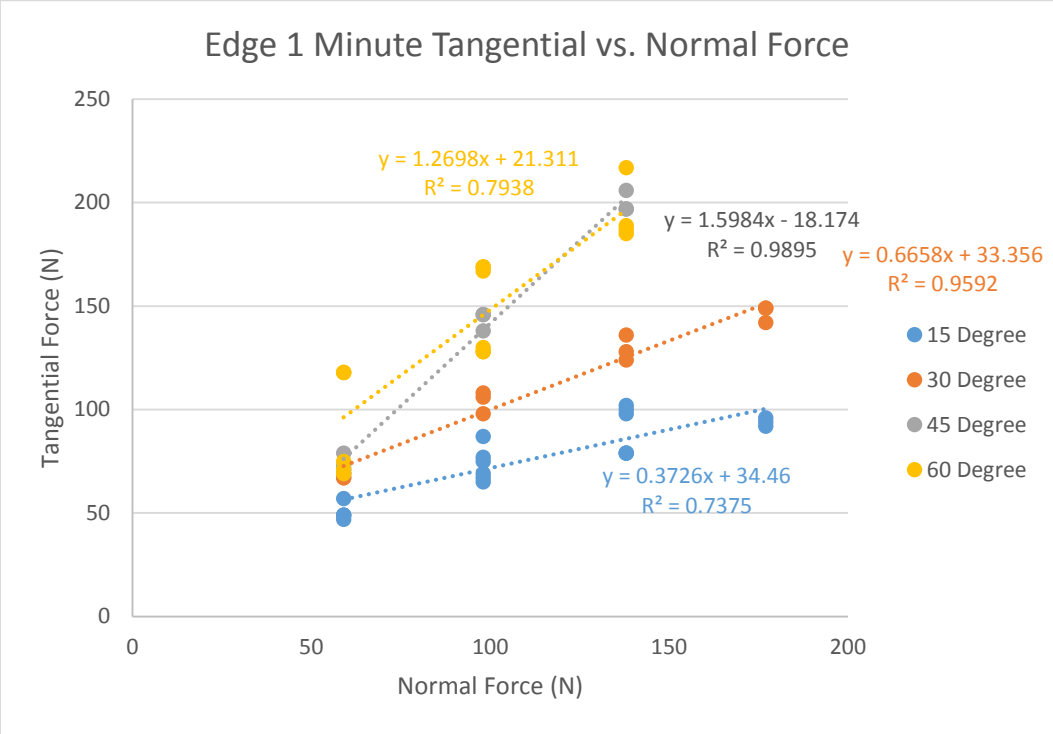

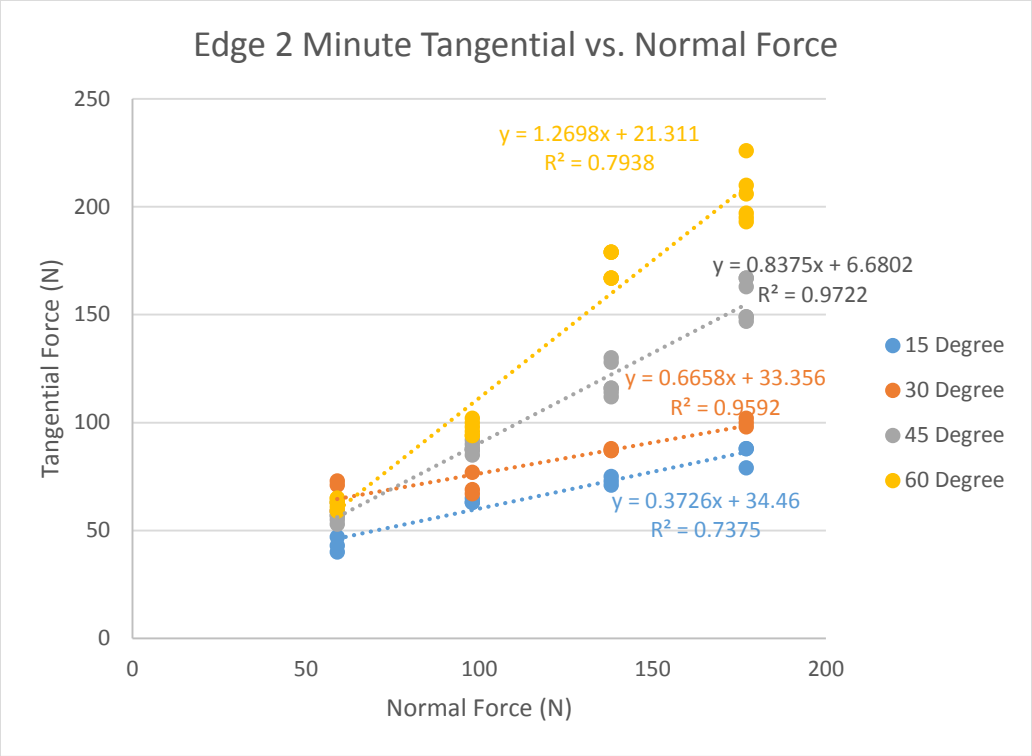
Edge 2 Minute Tangential vs. Normal Force
Tangential Force (N)
Normal Force (N)
0
50
100
150
200
250
y = 1.2698x + 21.311
R² = 0.7938
y = 0.8375x + 6.6802
R² = 0.9722
y = 0.6658x + 33.356
R² = 0.9592
y = 0.3726x + 34.46
R² = 0.7375
15 Degree
30 Degree
45 Degree
60 Degree

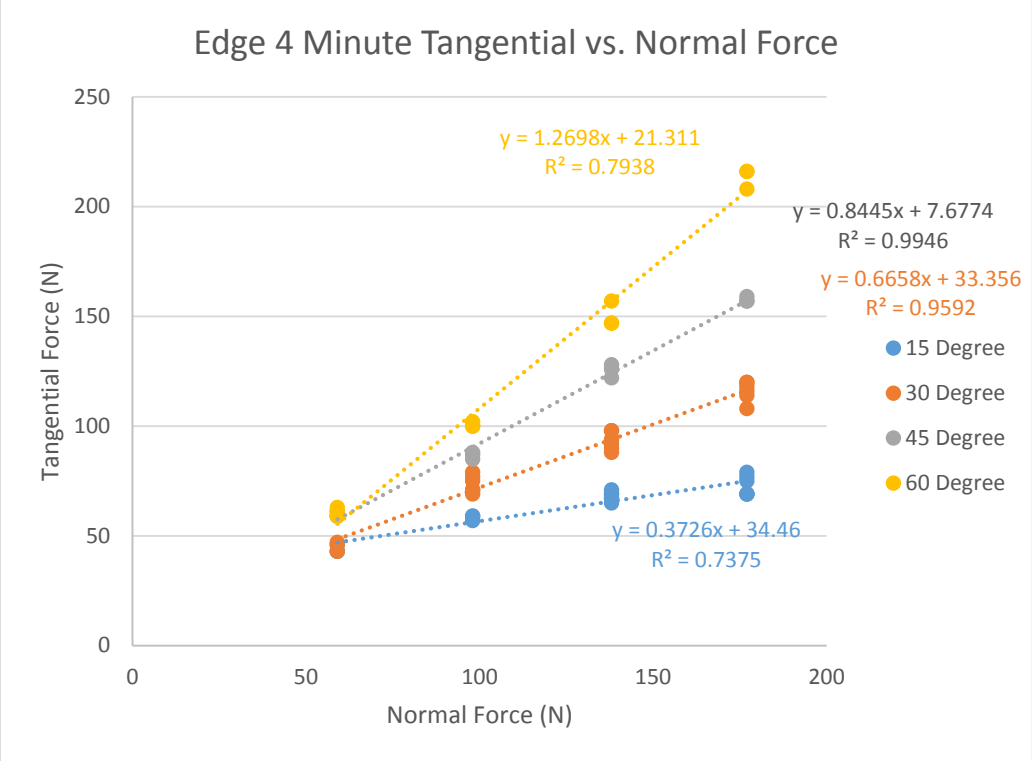
Edge 4 Minute Tangential vs. Normal Force
Tangential Force (N)
Normal Force (N)
0
50
100
150
200
250
y = 1.2698x + 21.311
R² = 0.7938
y = 0.8445x + 7.6774
R² = 0.9946
y = 0.6658x + 33.356
R² = 0.9592
y = 0.3726x + 34.46
R² = 0.7375
15 Degree
30 Degree
45 Degree
60 Degree

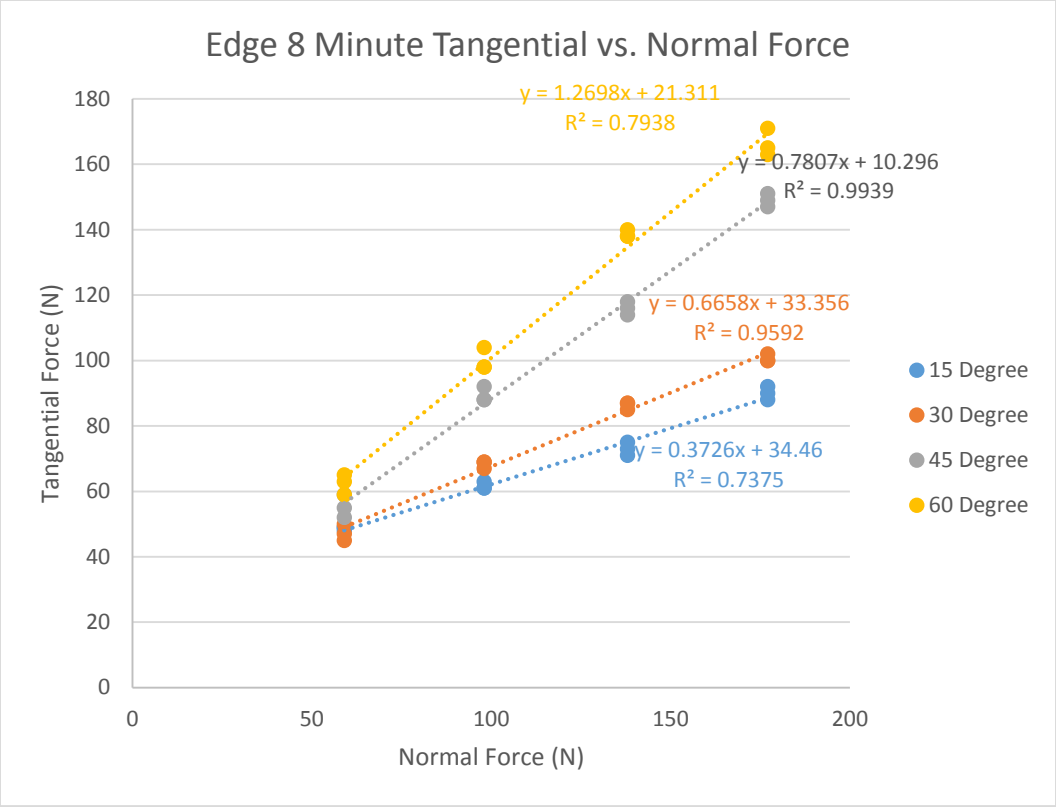

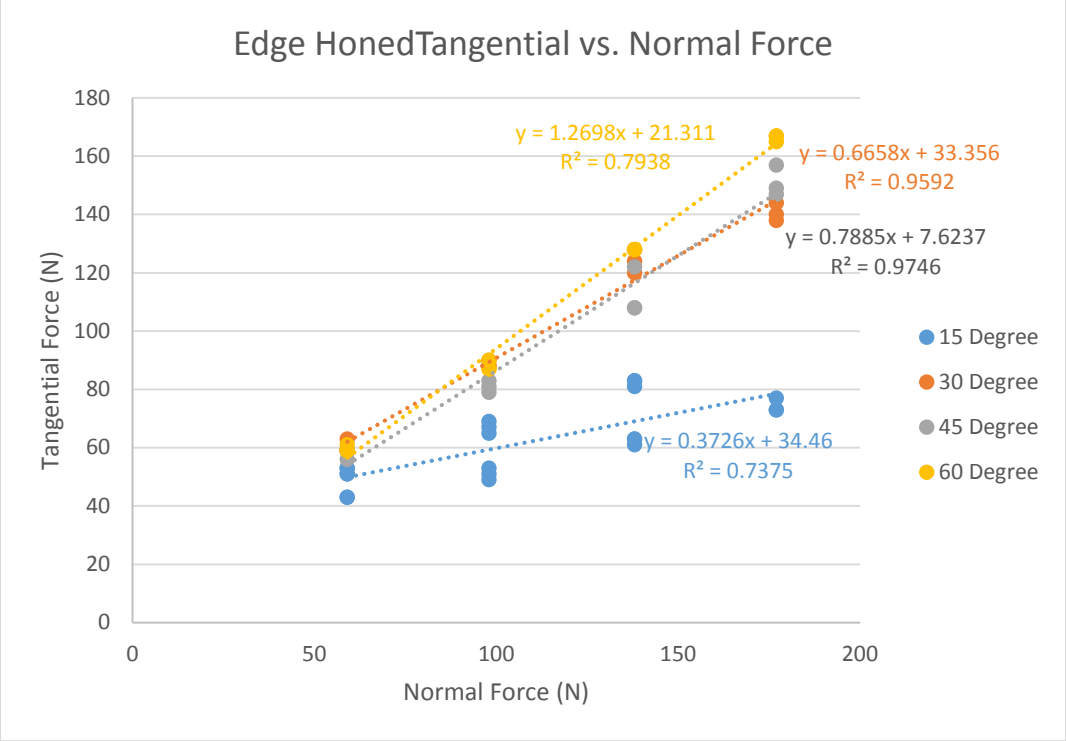

Appendix L: Previous Design Decomposition Iterations

2/18/2015:

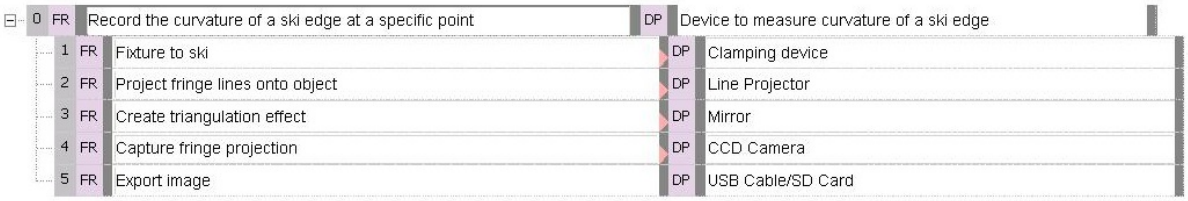

2/19/2015:

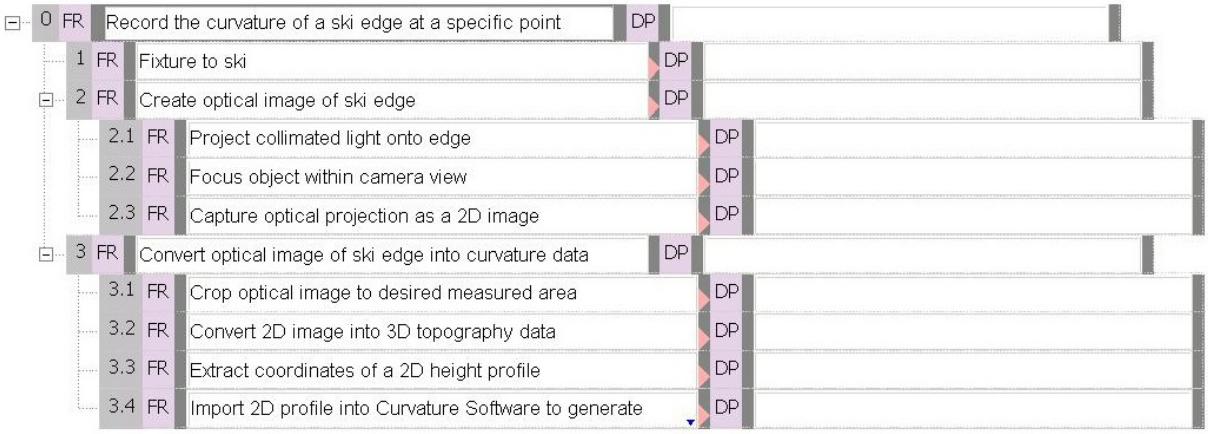

2/22/2015:

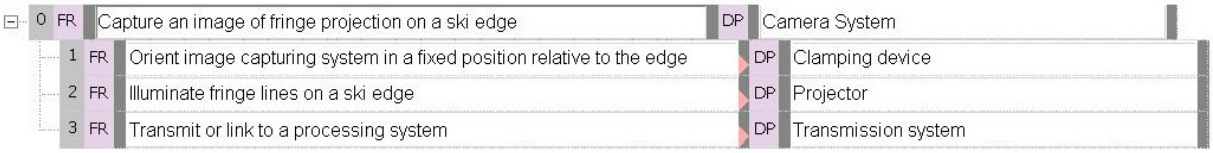

3/23/2015:

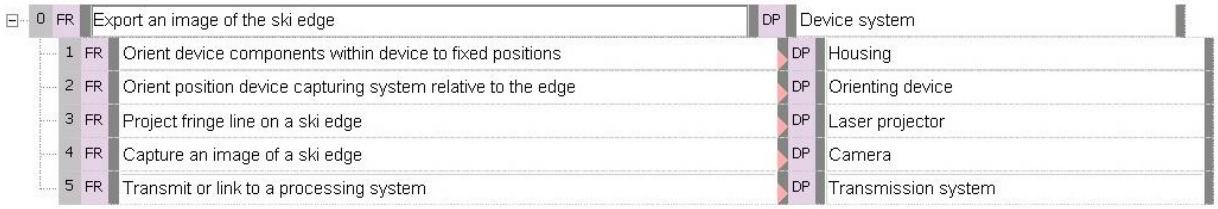

3/29/2015:

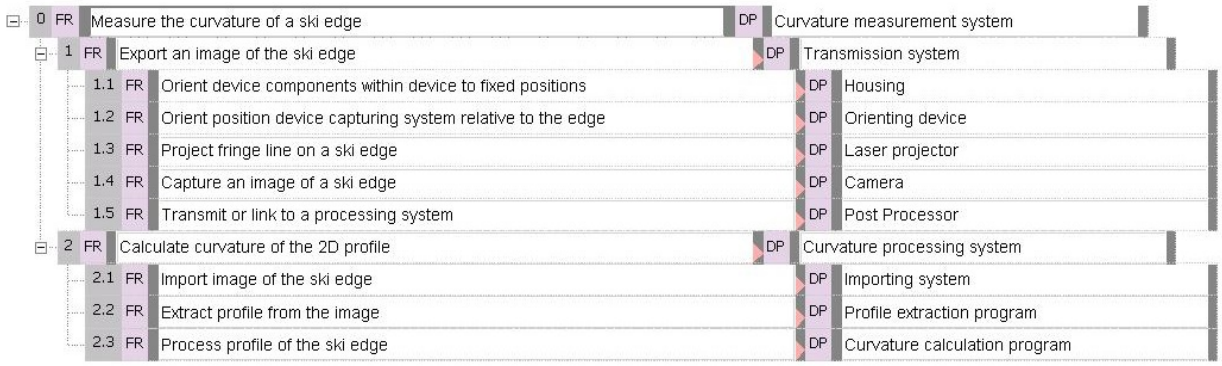

4/7/2015:

0	FR	Measure the curvature of a ski edge	DP	Curvature measurement system
1	FR	Acquire an image of the ski edge of sufficient resolution	DP	Transmission system
1.1	FR	Orient device components within device to fixed positions	DP	Housing
1.1.1	FR	Align laser over edge	DP	Fitting 1
1.1.2	FR	Align camera at projected line at 45 degree angler relative to the edge	DP	Fitting 2
1.1.3	FR	Hold device for stability	DP	Housing ouside contour
1.2	FR	Orient position device capturing system relative to the edge	DP	Orienting device
1.2.1	FR	Track the position of the device	DP	Laser trackier system
1.2.2	FR	Guide device along x axis	DP	Operator Movement
1.2.2.1	FR	Limit motion in y axis	DP	Roller
1.2.2.2	FR	Limit motion in z axis	DP	Roller
1.3	FR	Project fringe line on a ski edge	DP	Laser projector
1.4	FR	Capture an image of a ski edge	DP	Camera system
1.4.1	FR	Power on the camera	DP	Power system
1.4.2	FR	Magnify image	DP	Series of lenses
1.4.3	FR	Focus camera to edge	DP	Camera focus
1.4.4	FR	Signal for picture	DP	Impulse button
1.5	FR	Transmit or link to a processing system	DP	Post Processor
1.5.1	FR	Export image of ski	DP	Linking system
1.5.2	FR	Export position on ski	DP	Linking system
2	FR	Calculate curvature of the 2D profile	DP	Curvature processing system
2.1	FR	Import image of the ski edge	DP	Importing system
2.2	FR	Extract profile from the image	DP	Profile extraction program
2.3	FR	Process profile of the ski edge	DP	Curvature calculation program

Appendix M: Solid Model Iterations of Device Design

Corresponding files located at: \\research.wpi.edu\Surflab\2014-2015\Projects\Edge MQP\Appendix M

Iteration 1:

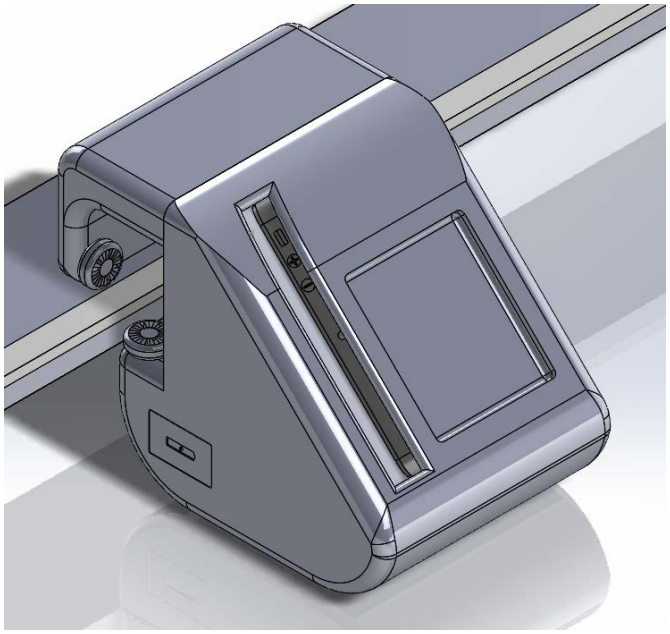

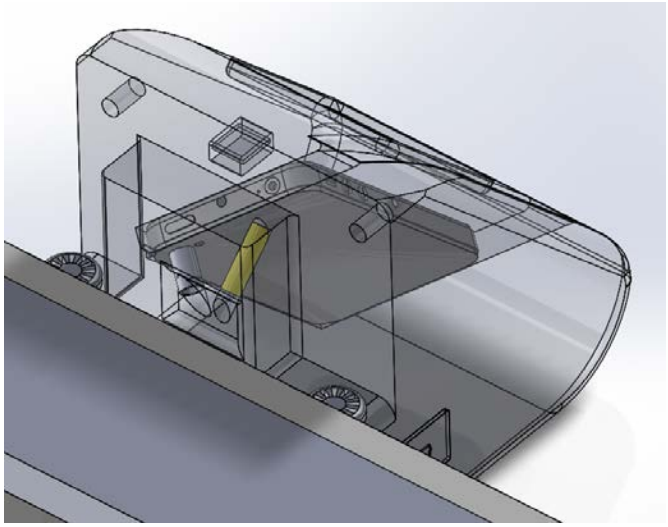

Iteration 2:

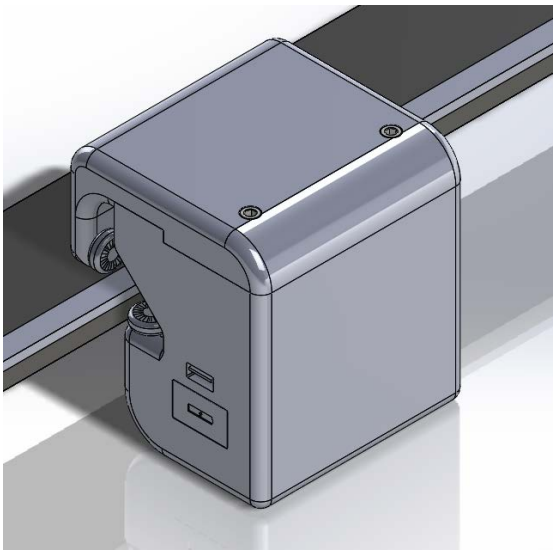

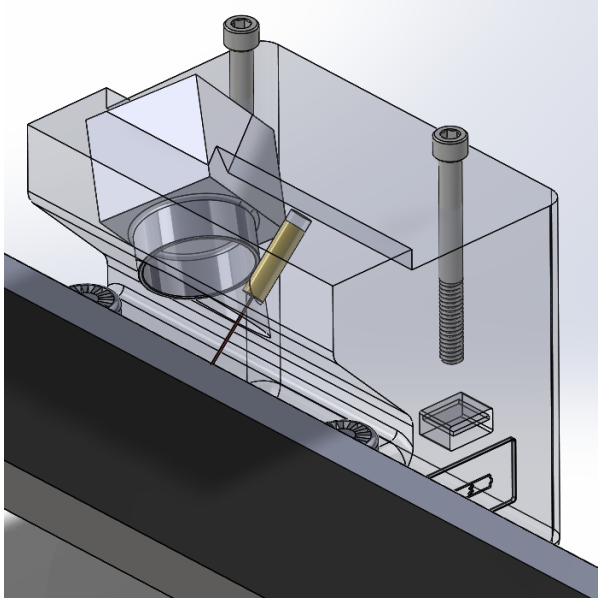

Appendix N: MATLAB Codes

Corresponding files located at: \\research.wpi.edu\Surflab\2014-2015\Projects\Edge MQP\Appendix N

image_reader

```
%Establishing a Function to read images
function [a] = image_reader(filename)

% User selected .jpg file
if(~exist('filename','var'))
    [fname, pname] = uigetfile('*.jpg','Please select the file');
    filename = sprintf('%s%s',pname, fname);
end

fid = fopen(filename,'r');

I = imread(filename);

a = imcrop(I);


end
```

MQP_Test_1:

```
clc; clear all; close all;
% Have a calibration function above
% Image Thresholding
[a] = image_reader();
imshow(a);
red = a(:,:,1);green = a(:,:,2);blue = a(:,:,3);
imshow(red);
% K = LineCurvature2D(Vertices,Lines);
d = impixel(a)
out = red > 250 & green>114 & blue > 149;
```

```
imshow(out)
out2 = imfill(out,'holes');
imshow(out2)
out3 = bwmorph(out2,'erode');
imshow(out3)
out4 = bwmorph(out3, 'dilate',2);
% Sobel and Canny Edge detection
b = rgb2gray(a);
Edge1 = edge(b,'sobel');
Edge2 = edge(b,'canny');
imshowpair(Edge1,Edge2,'montage')
BW4=edge(out3,'canny');
imshow(BW4)
BW5=imcrop(BW4);
figure(2);
imshow(BW5)
uiwait(msgbox('Locate the point'));
[x1,y1] = ginput(1)
[x2,y2] = ginput(1)
[x3,y3] = ginput(1)
sx = (x1 + x2 + x3)/2
sy = (y1 + y2 + y3)/2
scale = sqrt(sx^2 + sy^2)

hx = sqrt(sx*(sx - x1)*(sx - x2)*(sx - x3))
hy = sqrt(sy*(sy - y1)*(sy - y2)*(sy - y3))

khx = (4*hx)/(x1*x2*x3)
khy = (4*hy)/(y1*y2*y3)

kh = sqrt(khx^2 + khy^2)

radius = 1/kh

Pts = [x1, x2, x3; y1, y2, y3]

Int_Values = [sqrt(x1^2 + y1^2), sqrt(x2^2 + y2^2), sqrt(x3^2 + y3^2)]
```